THE EVOLUTION OF THE QUASAR CONTINUUM

NASA Grant NAGW-2201

Semiannual Report Nos. 1, 2, and 3

For the Period 1 July 1990 to 31 December 1991

Principal Investigator
Dr. M. Elvis

August 1992

Prepared for:

National Aeronautics and Space Administration
Washington, DC 20546

Smithsonian Institution
Astrophysical Observatory
Cambridge, Massachusetts 02138

The Smithsonian Astrophysical Observatory
is a member of the
Harvard-Smithsonian Center for Astrophysics

The NASA Technical Officer for this grant is G.R. Riegler, Code: SZE, National Aeronautics and Space Administration, Washington, DC 20546.

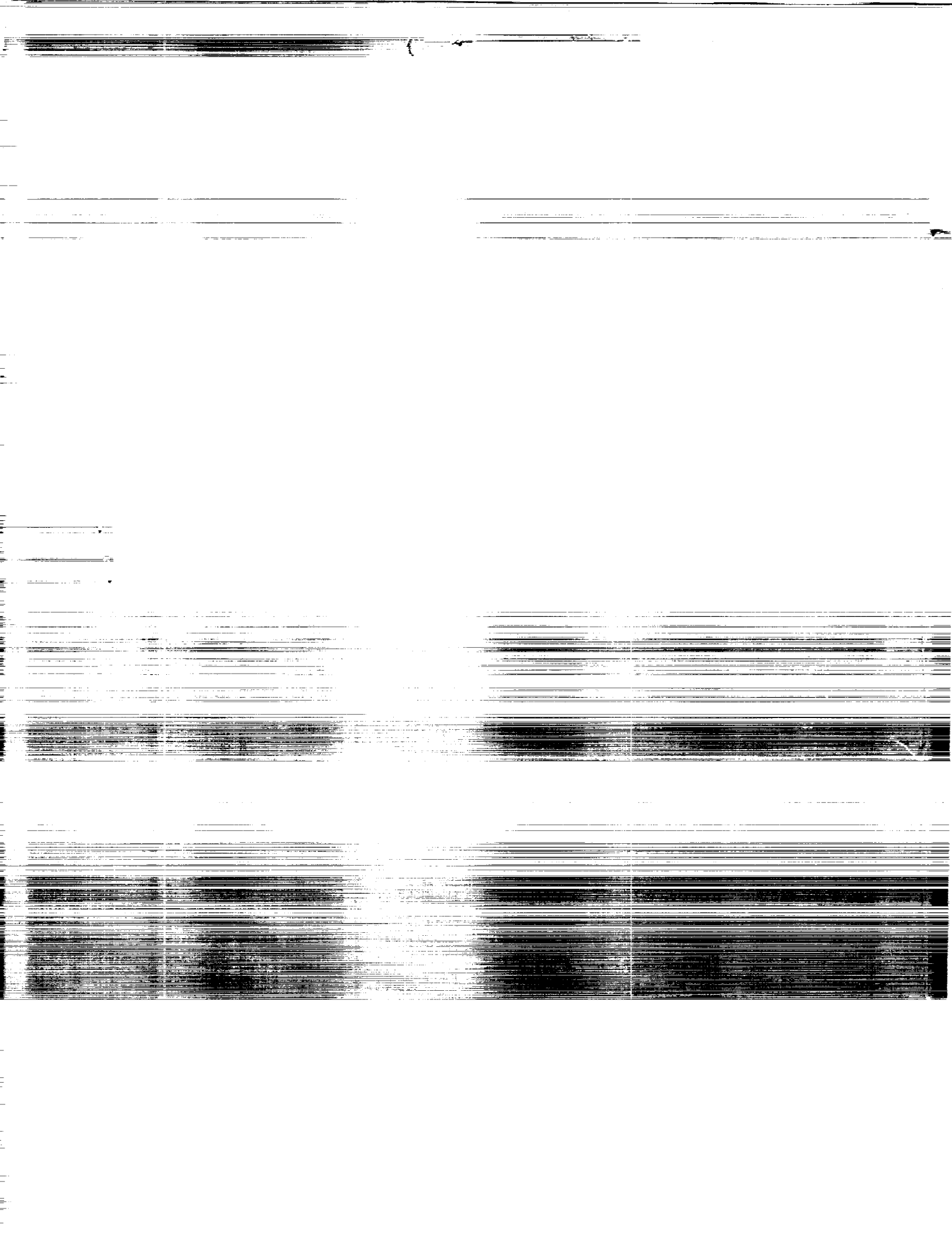

Contents

1 Introduction

The program of research supported by this grant has made tremendous progress since its inception. By having a long-term commitment of support it has been possible to plan a comprehensive program and use this as a means of defining supporting observational programs for a wide range of instruments, both space and ground-based.

We now have in hand a large data base of ROSAT data, optical and IR complementary data. We are the process of obtaining a large amount of IUE data for the same quasar sample. For our complementary sample att high redshifts, where the UV has been redshifted into the optical we have just had approved large amounts of observing time to cover the quasar continuum in the near-IR using new (NICMOS) array spectrographs. 10micron, optical, and VLA radio, data also have approved time. An ISO US key program has been approved to extend this work into the far-IR, and the launch of ASTRO-D (early in 1993) promises to extend it to higher energy X-rays.

This demanding observing program has not precluded the extraction of new science results as the data comes in: we have two ROSAT papers published and three more in preparation; the final Einstein IPC paper on quasar spectra has been submitted; a study of the limitations imposed by existing instrumentation is almost ready for submission; as is the foundational paper 'An Atlas of Quasar Continua'. Further details of these activities are given below. Followed by a summary of our plans for the coming year. First we outline the personnel supported by this project.

2 Personnel

This program supports: at SAO– two post-doctoral fellows, Dr. F. Fiore, and Dr. A. Siemiginowska, a research assistant C. Fassnacht, and provides partial funding for the P.I. and Dr. B. Wilkes; at Harvard– partial funding for a graduate student O. Kuhn (who also won her own NASA Graduate Research Studentship); at Univ. of Arizona– student support to assist Prof. J. Bechtold.

3 Research Progress

3.1 Einstein

The Atlas of quasar continua is complete (Elvis et al. 199). Host galaxy contributions have been tracked down for almost all objects. A point of importance on the variety of IR shapes was understood.

The influence of observing constraints in constraining the continuum shapes that can be seen was formalized during a visit to Bologna and a paper on the 'Spectral Window Function' is being prepared.

A database containing the results of the ROSAT analysis has been started.

The final Einstein IPC paper on quasar spectra was submitted to the Ap.J. (Shastri et al. 1992, see Appendix). It shows two new results: a dependence of X-ray spectral index on the radio 'core-dominance parameter' which probably reflects the importance of

the relativistically beamed 'jet' component in the X-ray spectrum; and a strengthening of the correlation of optical FeII emission line strength and X-ray spectral slope with more objects, especially for radio quiet quasars.

3.2 ISO

An ISO Key Project observing proposal "Exploring the Full Range of Quasar/AGN Properties" (P.I. B.Wilkes) was submitted to NASA and was approved. This program will provide a key extension into the far-IR for our multi-wavelength program for quasar continua. We are also working with Dr. Smith (NASM) on a program of quasar spectroscopy with the LWS on ISO that will give detailed continuum shapes for a small number of bright AGN.

4 ROSAT

When the first ROSAT PSPC spectrum of a high redshift ($z \sim 3$) quasar was obtained from the standard data processing pipeline at the GSFC RSDC it was immediately apparent that it had unexpectedly large absorption above the Galactic value. Subsequent analysis showed that this is likely (though not necessarily) intrinsic and is 10^{22} atoms cm^{-2}. At low z this would be a highly unusual state for a luminous quasar. Possible explanations include cold material in a relativistic jet, and evolutionary scenarios of the "shrouded quasar" type. A second high z quasar observation with ROSAT has been recieved and shows similar unexpected features as the first. The detection of X-ray absorption at high redshifts holds out the possibility of using X-ray spectroscopy to determine elemental abundances in the early universe more accurately and reliably than is now possible with UV and optical absorption line methods. A paper was submitted to Ap.J on this topic and has been published (Wilkes et al. 1992, see Appendix).

Extended X-ray emission was seen in the ROSAT HRI image of the classic type 2 Seyfert galaxy, NGC1068. The energy resolution of the HRI was used to show that this has a different spectrum from the nucleus. This result shows that spectra of AGN, at least at low luminosity, from instruments with $\leq$arcminute beam sizes cannot be assumed to be purely from a compact central object. A paper was submitted to Ap.J on this topic and has been published (Wilson et al. 1992, see Appendix).

ROSAT PSPC data on another quasar, 3C351, shows complex X-ray absorption. This may be explainable via a warm absorber, most likely in a flattened geometry seen nearly edge-on. A paper is in preparation on this subject.

Eight more high redshift ($z > 3$) quasars were detected in our ROSAT PSPC observations including one quasar at $z = 4.11$. Three have sufficient counts to provide an X-ray spectrum. All the objects have had their X-ray flux placed in a spectral energy distribution using data from Co-I J. Bechtold. Two papers are in preparation on this subject (Elvis, et al., Bechtold et al.).

Proposals for AO2 and AO3 were submitted, both from SAO and with Co-Is. Many of these were successful, and data from them will soon begin to arrive.

A database containing the results of the ROSAT analysis has been started.

Since several of our quasar observations have >10,000 counts we are becoming limited by systematic effects in the detector. Conversely our data can be used to help track down systematic problems. We have worked with MPE and the USRSDC to improve the PSPC spectral response matrix.

4.1 IUE

Seven IUE shifts were awarded to extend this study into the UV (PI: B. Wilkes). The first of this year's IUE observations was made on 1 June 1992, quasi-simultaneously with our ROSAT observation.

4.2 HST

An archival proposal (P.I. J. McDowell) was approved for access to the more than 25 HST spectra taken of objects in our Einstein/ROSAT samples. A proposal to complement a ROSAT program (P.I. A. Laor, Princeton) with new HST spectra has been submitted, concentrating on low z, low galactic N_H quasars to obtain the best constraints on the UV/soft x-ray big bump.

4.3 Ground-Based Observations

Our optical spectroscopy and near-IR (JHK) photometry made quasi-simultaneous with ROSAT continues. The MMT and 48-inch observations which were taken in support of the ROSAT program, and are being reduced. Our ROSAT and MMT observations of 3C351, the quasar with the warm absorber (see above), were taken, by chance, close in time to HST spectra of the same object. We have applied for archival access to these spectra.

We continue to participate in the NGC5548 monitoring campaign (Peterson et al. 1992) and have issued an IAU Circular on the results (Mathur and Kuhn 1992).

4.4 Selection of High Redshift Samples

Evolution studies demand well chosen samples for comparison. Definition of samples as a function of redshift for our project proceeds well. Two sets of quasars are being selected: constant luminosity, and constant evolved luminosity. A VLA proposal was submitted to determine the radio-loudness of the samples, and study the evolution of the fraction of quasars which are radio-loud.

Observing time at CTIO, MMT, SAO 48-inch and Steward 90-inch has been awarded for near-IR spectroscopy of high redshift quasars, with supporting optical spectroscopy, and an attempt to detect, or set good limits on, the mid-IR 10micron emission. These quasars have been carefully chosen to have strong overlap with our ROSAT and ISO programs.

4.5 Accretion Disk Models vs. Data

Work on accretion disk structure and comparison with the spectral energy distributions continues. A letter on the 'wall' in AGN accretion disks is being re-cast as two larger papers:

the first on the theory; the second on implications for observations. A paper comparing quasar optical/uv colors with simple disk and other theories is in preparation (Kuhn et al.). Modelling of the well monitored optical/UV outburst of GQ Comae in the color-color plane has also been performed and a paper submitted (Sitko et al. 1992). A second paper is in preparation.

4.6 Evolution via X-ray Source Counts

A collaboration to use the many serendipitous sources in our ROSAT observations to constrain the X-ray evolution of quasars and AGN has been established with B. Boyle of IoA, Cambridge, England. A first MMT proposal was submitted for the identification of these sources, and time was awarded.

5 Future Plans

With the observing program well in place, we will now concentrate on reducing and collating the vast amount of resulting data. Each separate part of the program can lead to results on its own and is being spearheaded by a particular individual. We expect the next 6 months to lead primarily to more ROSAT papers, since this data is in the most developed form.

New observing proposals will be written for ASTRO-D, and continuing proposals for the ground-based instruments. ROSAT AO-4 proposals are uncertain because of the supply of gas for the PSPC, but will be submitted if the instrument is in good health.

6 Bibliography

6.1 Refereed Papers

"The Soft X-ray emission in Einstein Quasar Spectra", Masnou, J.-L., Wilkes, B.J., Elvis, M., Arnaud, K.A., and McDowell, J.C., 1991, A&A, 253, 35.

"An X-ray Image of the Seyfert Galaxy NGC 1068" A.S. Wilson, M. Elvis, A. Lawrence, and J. Bland-Hawthorn, 1992, Ap.J.(Letters), 391, L75.

"PKS0438-436: A High Redshift Quasar with Strong X-ray Absorption", B.J. Wilkes, M. Elvis, H. Tananbaum, J.C. McDowell, and A. Lawrence, 1992, Ap.J.(Letters), 393, L1.

"Steps towared determination of the size and structure of the Broad-line Region in AGN. III: Further observations of NGC5548 at optical wavelengths", B.M.Peterson etal (34 authors, incl. Elvis, Wilkes), 1992, Ap.J., 392, 470

"Multifrequency observations of the Optically Active, Radio-Quiet Quasar GQComae: II. Nature of the Continuum Variability", Sitko., M.L., Sitko, A.K., Siemiginowska, A., Szczerba, R., Ap.J., submitted.

"Quasar X-ray Spectra Revisited" Shastri P., Wilkes, B.J., Elvis, M., McDowell, J.C. 1992, Ap.J., submitted.

6.2 IAU Circular

"NGC5548", S. Mathur, O. Kuhn 1992, IAU Circular 5535.

6.3 Published Conference Proceedings

"The Spectral Window Function and the Extremes of Quasar X-ray Spectra", M. Elvis, 1992, in "Frontiers of X-ray Astronomy", ed. Y. Tanaka and K. Koyama [Universal Academic Press], p. 567.

"Optical Variability from a Thermally Unstable Region in AGN Accretion Disks", A. Siemignowska, M. Elvis, O. Kuhn, and B.J. Wilkes, 1991, in "The Physics of Active Galactic Nuclei", eds. W.J. Duschl and S.J. Wagner, [Springer Verlag], p.

"Quasar X-ray Spectra Revisited", P. Shastri, B. Wilkes, M. Elvis, and J. McDowell, 1991, in "The Physics of Active Galactic Nuclei", eds. W.J. Duschl and S.J. Wagner, [Springer-Verlag], p.

"The ROSAT X-ray Spectrum of PG1426+015", B.J. Wilkes, M. Elvis, J. McDowell, and A. Lawrence, 1991, in "The Physics of Active Galactic Nuclei", eds. W.J. Duschl and S.J. Wagner, [Springer-Verlag], p.

"A Thermal Model of the Continuum Variability of GQ Comae (PG1202+281)", Siemiginowska, A., Sitko, M., 1991, in: "Physics of AGN",Proceedings of Conference in Heidelberg, in press.

"Using Color-Color Diagrams to Test Models for the 'Blue Bump' ", O. Kuhn, J.C. McDowell, M. Elvis, and B.J. Wilkes, 1992, in "Testing the AGN Paradigm", eds. S.S.Holt, S.G.Neff and C.M. Urry, p.208.

"Infrared Weak Quasars", J.C. McDowell, M. Elvis, and B.J. Wilkes, 1992, in "Testing the AGN Paradigm", eds. S.S.Holt, S.G.Neff and C.M. Urry, p.532.

"Star-disk collisions in Active Galactic Nuclei and the origin of the Broad Line Region", Zurek, W.H., Siemiginowska, A., Colgate, S., 1992, in 'Testing the AGN Paradigm, eds. S.S.Holt, S.G.Neff and C.M. Urry, p.564

"ROSAT X-ray Spectra of Quasars with a Range of Continuum Properties and Redshift", B.J. Wilkes, M. Elvis, H. Tananbaum, J.C. McDowell, and A. Lawrence, in "AGN and X-ray Background",, 1992, ed. [MPE Nov. 1991], in press.

"Multifrequency Observations of Kaz 102 during ROSAT All Sky Survey", A. Treves, H.H. Fink, M. Malkan, L. Maraschi, M.-H. Ulrich, W. Brinkmann, D. deMartino, M. Elvis, J. Heidt, J. McDowell, S. Schaeidt, E.G. Tanzi, S. Wagner, and B. Wilkes, 1992, in "X-ray Emission from AGN and the Cosmic X-ray Background", ed. , in press.

"ROSAT Spectra of Quasars with Substantial Redshifts", M. Elvis, B.J. Wilkes, H. Tananbaum, A. Lawrence, and J. McDowell, 1991, BAAS, 23, No.4, 1344.

"Infrared Weak Quasars", J. McDowell, M. Elvis, B.J. Wilkes, O. Kuhn, 1991, BAAS, 23, No.4, 1424.

"The Relationship between Quasar Emission Lines and Their UV/X-ray Continuum Properties", 1991, S. Mathur, B.J. Wilkes, M. Elvis, and J. McDowell, BAAS, 23, No.4, 1424.

"Recent ROSAT Results on High Z Quasars", 1992, B.J. Wilkes, 33rd Herstmonceux Conference, in press.

6.4 ReportsOB/Popularizations

"Quasar Energy Distribution Conference" summary, 1992, B.J. Wilkes, SERC Newsletter.
"Emerging Pictures of Quasars", B.J. Wilkes, Astronomy Magazine, Vol. 19, #12, p34.
"Quasars", CfA Public night talk, B.J. Wilkes, Feb 1992.

6.5 Talks, Presentations

"The Spectral Window Function", M. Elvis, Colloquium, October 1991, Univ. of Bologna (Italy)

"The spectral window function and the true range of quasar continuum shapes" M. Elvis, November 1991, seminar, U.Md

"ROSAT Results on AGN and Quasars" M. Elvis, January 1992 invited talk at "Signatures of Black Holes and Neutron Stars", Workshop at the Aspen Center for Physics.

"Recent Developments in X-ray Astronomy of Quasars" M. Elvis, May 1992, 2nd New England Regional AGN meeting, invited review.

"The High Energy View of Quasars", M. Elvis, invited review at APS meeting, April 1992 DC.

"Quasar Energy Distributions", J. McDowell, MSFC Space Science Lab, 1990

"Ultraviolet and X-ray Observations of Quasars", J. McDowell, CITA, 1991

"Continuum Energy Distributions of Quasars", J. McDowell, Barnard College, NY, 1990.

"Continuum Energy Distributions of Quasars", J. McDowell, Physics Dept, U. of Wisc.-Madison, Oct 1990.

"The Relationship Between Quasar Emission Lines and Their UV/X-ray Coninuum Properties", S. Mathur, May 1992, New England Regional Meeting, Haystack Observatory.

"The X-ray Variability of the Seyfert Galaxy NGC 6814" F. Fiore, May 1992, Haystack meeting, Second New England Regional Quasar/AGN Meeting.

'Thermal Continuum Emission of AGN.' A. Siemiginowska, 1990: Hubble Space Telescope, Baltimore

'Thermal Emission from AGN: Theory and Observations' A. Siemiginowska, 1991, University of Cincinnatti

'Thin Accretion Disks in AGN: theory and observations' A. Siemiginowska, 1991, Los Alamos National Laboratory

'Star-disk interactions and the origin of BLR', A. Siemiginowska, 1992, Warsaw, Poland

'Time-Evolution of Thin Accretion Disks in AGN' A. Siemiginowska, 1992, ESA, Garching Germany.

'AGN - what we know about them?' A. Siemiginowska, 1992, Los Alamos Nationsl Laboratory

Ph.D. talk in December 1991, A. Siemiginowska, Warsaw, Poland 'Thin Accretion Disks in AGN: theory and observations'

" Quasar Continua", B.J. Wilkes, 1990, IoA conference on BLRs in Cambridge

"ROSAT Quasar Spectra", B.J. Wilkes, 1990, Heidelberg
"ROSAT Quasar Spectra" including PKS0438,0439, B.J. Wilkes, 1991, Heidelberg
"PKS0439", B.J. Wilkes, 1991, AAS.
AAS Poster, Shastri et al. 1991, AAS.
"Quasar Energy distributions", B.J. Wilkes, 1991, Colloquium at Boston University.
"Quasar Energy distributions", B.J. Wilkes, 1992, Colloquium at University of Pittsburg.
"Quasar Energy distributions", B.J. Wilkes, 1990, Colloquium at MIT.

A Papers

Harvard-Smithsonian Center for Astrophysics

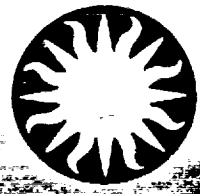

Preprint Series

No. 3410

(Received April 20, 1992)

PKS0438-436: A HIGH REDSHIFT QUASAR WITH STRONG X-RAY ABSORPTION

Belinda J. Wilkes, Martin Elvis, Fabrizio Fiore, Jonathan C. McDowell, and Harvey Tananbaum
Harvard-Smithsonian Center for Astrophysics

and

Andrew Lawrence
Department of Physics, Queen Mary and Westfield College, London

To appear in
The Astrophysical Journal (Letters)

HARVARD COLLEGE OBSERVATORY SMITHSONIAN ASTROPHYSICAL OBSERVATORY
60 Garden Street, Cambridge, Massachusetts 02138

Center for Astrophysics
Preprint Series No. 3410

PKS0438-436: A HIGH REDSHIFT QUASAR WITH STRONG X-RAY ABSORPTION

Belinda J. Wilkes, Martin Elvis, Fabrizio Fiore, Jonathan C. McDowell, and Harvey Tananbaum
Harvard-Smithsonian Center for Astrophysics

and

Andrew Lawrence
Department of Physics, Queen Mary and Westfield College, London

PKS0438-436: A HIGH REDSHIFT QUASAR WITH STRONG X-RAY ABSORPTION.

Belinda J. Wilkes[1], Martin Elvis[1], Fabrizio Fiore[1],
Jonathan C. McDowell[1], Harvey Tananbaum[1] and Andrew Lawrence[2]

April 15, 1992

[1] Harvard-Smithsonian Center for Astrophysics, 60 Garden Street, Cambridge, MA02138
[2] Department of Physics, Queen Mary and Westfield College, Mile End Road, London E1 4NS

1 Abstract

We report the first X-ray spectrum of a high redshift (z=2.85) quasar. The ROSAT PSPC spectrum of PKS0438-436, covering 0.3-9 keV in the quasar's rest frame, reveals unexpected absorption of $\sim 1 \times 10^{22}$ cm^{-2} assuming it occurs at the source. Only one other high luminosity quasar (of $\gtrsim$50 observed by *Einstein*) shows significant absorption in its X-ray spectrum. Of the common line-of-sight absorbers, only highly ionized Lyman α forest clouds may be able to explain this amount of absorption. Candidates for an intrinsic absorber are discussed. Absorption at ~1keV (rest frame) is due primarily to heavy elements (O,Ne,Mg,Si,S) raising the possibility of measuring early universe abundances via X-ray absorption in this and like quasars. PKS0438-436 may be a high redshift member of a population of quasars which can contribute to the X-ray background above 2keV, without being detectable by previous imaging missions.
Keywords: quasars: individual: PKS0438-436

2 Introduction

X-ray spectral observations of quasars have been confined to low redshift objects ($z \leq 0.5$) whose proximity makes them bright enough to study. ROSAT, with its high sensitivity, enables us to observe the spectra of high redshift ($z > 2$) quasars for the first time. The first quasar observed in our program has given an unexpected result in that, unlike low redshift quasars, it has significant absorption in its X-ray spectrum.

Only two quasars of the $\gtrsim$50 studied with *Einstein* (Wilkes & Elvis 1987, Canizares & White 1989, Worrall & Wilkes 1989) are known to have strong, soft X-ray absorption, variable in both cases: MR2251-178 (Halpern 1984, Pan, Stewart and Pounds 1990), with an X-ray luminosity of $\sim 4 \times 10^{44}$ergs^{-1} (0.5-4.5 keV rest frame, Wilkes *et al.* 1992), and NRAO140 (Marscher 1988, Turner *et al.* 1991), X-ray luminosity $\sim 1 \times 10^{46}$ergs^{-1} (2-8 keV). In all other cases there is no detectable absorption in excess of the Galaxy, and frequently

the presence of a soft excess results in a fitted N_H less than the Galactic value when a single power law spectral form is assumed (Wilkes & Elvis 1987). The possible presence of a soft excess adds to the uncertainty in the column density but values above a few $\times 10^{20}$cm^{-2} are unlikely since they would imply an extremely strong soft excess. Significant absorption ($\sim 10^{22}$cm^{-2}) has been seen in low luminosity active galaxies ($\lesssim 10^{43}$ergs^{-1}) and it has been suggested (Lawrence & Elvis 1982, Reichert *et al.* 1985, Kruper, Urry & Canizares 1990) that the amount of intrinsic absorption in active galaxies is inversely related to luminosity, an obvious interpretation being that the higher luminosity central source ionizes and clears out a larger portion of the host galaxy.

3 Observations and Analysis

PKS0438-436 was selected as a high-redshift ROSAT target based on its high *Einstein* flux compared with other similar redshift quasars in the *Einstein* databank (Wilkes *et al.* 1992). It is a radio-loud, core-dominated, highly polarized (Impey & Tapia 1988) quasar (Table 1). The ROSAT/PSPC observation was made with the source at the field center and the spacecraft wobble turned off (not by design) resulting in a poorly determined flux due to the unknown proportion of the observation for which the source lay under a window support wire. The source spectrum, the subject of this paper, is not affected. Counts were extracted from a 1.5′ radius circle centered on the source centroid, with background estimated within an annulus of inner and outer radii 2′ and 4′ respectively. The full-width at zero intensity of the source is observed to be 1.5′ and thus a circle with this radius contains $\gtrsim$95% of the counts, those lost being due to mirror scattering over the whole field. The 34 energy channels used by the MPE SASS pipeline processing were used in this analysis.

In order to provide a simple characterization of the source spectrum, a single power law with free, local N_H was fitted to the observed spectrum yielding $\alpha_E=0.8^{+1.5}_{-0.3}$, $N_H=7.8^{+26.1}_{-2.6} \times 10^{20}$cm^{-2} with a reduced $\chi^2=0.88$ (1σ errors, 2 interesting parameters (pars), channels 5:34[1]). The latest version of the PSPC response matrix was used for this fit, *i.e.* that released in February 1992 and recently installed in the SASS processing system (Snowden *et al.* 1992). The level of uncertainty in this matrix is $\lesssim$4% based on fits to the Crab and HZ43 calibration data (Snowden, private communication), insignificant when compared with $\sim$ 20 % statistical errors per channel in the current spectrum. The best fit spectrum is shown in Figure 1a with the data superposed and the residuals beneath. Figure 1b shows the 68%, 90% and 99% α_E, N_H confidence contours for the fit. We note that, while the data do not require a spectrum more complex than this simple power law, it is not a unique fit to the data but rather a convenient and simple representation.

As noted above, due to the lack of spacecraft wobble for this observation, estimates of the source flux are unreliable as the fraction of the observation for which the source may have been occulted by one of the window support wires is uncertain. The count rate for our target is low (~ 0.06 s^{-1}) so that its light curve shows no clear indication of such occultation. The flux indicated by the spectral fits is 1.5×10^{-12}erg cm^{-2}s^{-1} (0.1-2.5 keV) but could be as high as twice this value.

The equivalent neutral hydrogen absorbing column density, determined under the assumption of solar abundances based on the amount of metal absorption observed in the X-ray spectrum, is significantly larger than the measured Galactic column (Figure 1b). A second

[1]Channels 1:4 contain no significant signal.

quasar in the same PSPC field, PKS0439-433 (Table 1), shows a spectrum, with similar signal-to-noise (S/N), consistent with the Galactic column density (Figure 1b, α_E=1.4±0.3, N_H=$2.3^{+0.8}_{-0.7}$, χ^2=0.73, channels 1:34, 1σ, 2 pars.)[2]. The spectrum of the subtracted background is similar for both quasars. This result precludes the presence of an additional local absorber or of systematic effects in the data itself [3]. We conclude that the excess absorption in the spectrum of PKS0438-436 must lie either outside our Galaxy along the line-of-sight, or be intrinsic to the quasar. The amount of material implied depends on the redshift at which it is situated. If it is intrinsic, the rest frame energy range seen by ROSAT is 0.3-9 keV with the spectrum absorbed up to 2 keV. A spectral fit with local absorption fixed at the measured Galactic value plus free absorption at z=2.85 yields no change in slope (α_E=$0.7^{+0.7}_{-0.3}$) and an intrinsic absorption column of $1.0^{+0.7}_{-0.4} \times 10^{22}$cm^{-2} (reduced χ^2=0.83, Figure 2a). We then made a series of spectral fits with two absorbing components, one fixed at the Galactic column density with redshift zero[4], and the second free to vary and placed at a range of redshifts up to 2.85. The resulting dependence of the deduced column density of the absorber upon its redshift is shown in Figure 2b.

4 Results

PKS0438-436 with an X-ray luminosity in the range $1.7 \pm 0.1 \times 10^{47}$ergs^{-1} (*Einstein*, 0.5-4.5 keV, Wilkes *et al.* 1992) $\sim 3-6 \times 10^{47}$ergs^{-1} (ROSAT) is the highest luminosity quasar with significant soft X-ray absorption. Along with NRAO140, it does not follow the previously reported inverse correlation between luminosity and X-ray absorption unless the absorption should prove to be along the line-of-sight rather than intrinsic to the quasar.

PKS0438-436 was also observed by the *Einstein* Observatory on 26 August 1979. 160±18 counts were detected and, with a flux of $9.0\pm0.1 \times 10^{-13}$erg cm^{-2} s^{-1} (0.16-3.5 keV, Wilkes *et al.* 1992), was one of the brightest, high redshift quasars observed. This flux level is $\sim$ half that seen by ROSAT suggesting variation as the ROSAT value is probably a lower limit. The S/N of the observation is too poor to obtain a constraint on the spectral parameters beyond local $N_H \lesssim 2 \times 10^{22}$cm^{-2}, although the best fit value of $N_H \sim 8 \times 10^{20}$cm^{-2} is comparable with the value from ROSAT (Canizares & White 1989).

The X-ray energy spectral index of PKS0438-433 ($\alpha_E \sim 0.8$) is consistent with those observed for radio-loud and highly polarized quasars (Wilkes & Elvis 1987, Worrall & Wilkes 1989). However it is flatter than the typical 1.2 energy index recorded, mostly for radio-quiet quasars, by ROSAT (Brinkman *et al.* 1992). There is some evidence from ROSAT in both survey and deep pointed data that the quasar spectral slopes flatten towards higher redshift (Brinkman *et al.* 1992, Shanks *et al.* 1991).

The presence of a strong absorber is not a unique interpretation of these observations. Instead the spectrum may be complex, for example with spectral flattening towards lower energies, as observed in BL Lac objects (Madejski *et al.* 1992). A broken power law fit to PKS0438-436 gives a break energy of 0.9±0.2 keV and a low energy slope $\alpha_E = -1.2 \pm 0.6$ (χ^2=0.81, no significant improvement over a single power law model). The extreme change in slope ($\Delta\alpha \sim 2$ c.f. 0.7 for BL Lacs) and the higher break energy (3.0 c.f. 1.5 keV, rest

[2]We note that the PKS0439-433 data show no indication of the presence of a soft excess and no good fit could be found with a broken power law model, $\chi^2_{min} \sim 50$.

[3]The light curves of PKS0438-436 show no systematic effects which could lead to the observed absorption.

[4]Allowing the local absorber to be free results in no useful constraints on the spectral parameters. The best fit values do not change significantly.

frame), along with the lack of any similar observations for other flat-spectrum, radio-loud quasars make this an unlikely interpretation.

5 Identity of the Absorber

The ROSAT/PSPC spectral resolution does not allow us to distinguish between excess absorption along the line-of-sight or intrinsic to the quasar so both possibilities are considered.

5.1 Line-of-sight Absorption

Absorption along the line-of-sight to quasars is a well-known and heavily studied phenomenon with "Lyman α forest" and metal line systems being the dominant sources. The former typically have low neutral hydrogen column densities ($\sim 10^{14}\mathrm{cm}^{-2}$) which, even integrated over $\Delta z \sim 3$, cannot explain that observed in the soft X-ray. Their uncertain level of ionization, with estimates of the neutral to ionized gas ratio as low as $10^{-5} - 10^{-6}$ (Chokshi 1992), narrows the discrepancy but the lack of metal absorption lines is inconsistent with the strong metal absorption in the X-ray. The higher column density ($\sim 10^{18}\mathrm{cm}^{-2}$) metal line systems, with ionization $\sim 10^{-3}$, are a stronger possibility but their much lower density, ~ 1.2 per redshift interval (Sargent, Steidel and Boksenberg 1989), again falls short of the X-ray measurements.

Higher column density absorbers which are also fairly common are the Lyman α disk systems (characterized by damped Lyα absorption lines, see Turnshek *et al.* 1989 and references therein). The optical spectrum of PKS0438-436 shows no strong Lyman α absorption down to 3500 Å (*i.e.* z=1.88, Morton, Savage & Bolton 1978) so that any such system must be situated at z<1.88. Searches for Lyman α disk absorption have indicated that such systems, typically with column densities $\sim 10^{20} - 10^{21}\mathrm{cm}^{-2}$, occur at the rate of dN/dz = 0.29 $\pm$0.07 (Turnshek *et al.* 1989). Thus, if we assume that there is no evolution in Lyman α disk systems, there is a 55% chance of one existing at z< 1.88 along the line of sight to PKS0438-436. Given that a single system would provide insufficient column density unless it is at z<0.4 (Figure 2b) and that all systems found to date are at z$\sim$ 2, it seems unlikely that Lyman α disks are responsible for the absorption we see.

Another possibility for absorption along the line-of-sight is the presence of dust in intervening galaxies which has been suggested to account for the lack of high redshift quasars in current surveys (Heisler & Ostriker 1988). However the prediction is that, for quasars brighter than 22 magnitude, the reddening is minimal. Specifically at z=2.85, the predicted mean absorption has $E_{B-V} \sim 0.15 \pm 0.13$ while the N_H we observe indicates E_{B-V} of ~ 1, a $\sim 6\sigma$ deviation above this. The presence of dust in intervening galaxies is unlikely to explain the large column in PKS0438-436.

5.2 Intrinsic Absorption

The alternative of intrinsic absorption may be related to its high redshift, high luminosity or the apparent importance of beaming. Little previous X-ray spectral information exists for any of these regimes. Typical intrinsic X-ray column densities seen in low luminosity active galaxies are also $\sim 10^{22}\mathrm{cm}^{-2}$ so that the detection of a similar column in a high luminosity object may not be surprising. If PKS0438-436 were at low redshift the absorption would have reduced its soft X-ray flux by a factor ~ 10, so that an object with comparable bolometric

flux would not have been detected by *Einstein* or ROSAT. The lack of observations of such systems to date could be a selection effect due to the higher X-ray flux limit of previous missions.

PKS0438-436 has no broad absorption lines, ruling out a broad absorption line cloud as an absorption candidate. It does have broad emission lines, so a cloud in this region, which would have roughly the correct column density ($2.5 \times 10^{22} \mathrm{cm}^{-2}$, Kwan & Krolik 1981) is a possibility. However their typical size, $\sim 10^{13}$ cm, is likely smaller than the X-ray source implying partial covering. Leakage of soft photons would then be expected whereas the X-ray spectrum shows no evidence for this, a covering factor of > 0.8 is required. The absorbing cloud must therefore be larger than the typical broad line region cloud.

Both PKS0438-436 and NRAO140 have very strong, core-dominated, radio emission and high optical polarization implying relativistic beaming towards us. Naïvely one would expect such objects to be less likely to contain intrinsic absorbing material along our line-of-sight. However, the BL Lac object PKS2155-304, which has many similar properties, also has unexpected X-ray absorption (Canizares & Kruper 1984), as do other BL Lacs (Madejski *et al.* 1991,1992). This absorption has been identified as an OVIII Lyα absorption feature at low redshift ($z < 0.15$ for PKS2155-304) from hot ($\sim 10^6$ K) or highly ionized material with a column density of $2 \times 10^{22} \mathrm{cm}^{-2}$. The material is likely to be situated in or close to the beam of the radio source and is required to be in this very hot or very highly-ionized state due to the presence of only a single absorption line. The absorption in PKS0438-436 is broad and shows no evidence for recovery at low energies, implying cooler material ($\lesssim 10^6$ K for coronal ionization and $\lesssim 10^4$ K for photoionization equilibrium, Kallman & Krolik 1986). Alternatively, as suggested by the referee, the material could be highly ionized and have very high velocities ($\sim$0.8c) generating a broad absorption line analogous to those in BAL quasars. The absorption in PKS2155-304 has a width of $\sim$ 0.1c.

If the intrinsic absorption is evolutionary (*i.e.* due to its high redshift), PKS0438-436 may be a high-redshift analogue of the ultra-luminous infrared galaxies discovered by IRAS (Sanders *et al.* 1988). These are suggested to be young quasars in a dust-enshrouded initial phase. The E_{B-V} values deduced from the emission line ratios for the IRAS galaxies are in the range 0.6$-$2.3, in good agreement with the X-ray column density of PKS0438-436.

With only one high redshift quasar observed, it is impossible to distinguish between these various candidate absorbers. Clearly X-ray spectra of more objects are required to further study this phenomenon.

6 Discussion

It seems likely that the strong, soft X-ray absorption is intrinsic to PKS0438-436. Whether intrinsic/extrinsic, its discovery at high redshifts provides us with a new opportunity to study the metallicity of gas since X-ray absorption is strongly metal sensitive. Optical lines in emission or absorption, the only metallicity indicator to date, have proved unreliable due to uncertainties in the ionization conditions and to saturation and blending of the lines. The X-ray absorption column is, however, a direct measure of the K edge strengths of O,Ne,Mg,Si,S,Fe and is insensitive to ionization state as long as the gas is not fully ionized. With higher resolution spectra the edges of the individual elements can be measured. From the current observation alone we cannot place limits on the evolution of the metallicity with redshift since we have no independent measure of the hydrogen column density although we can conclude, unsurprisingly given quasar emission lines, that metals exist at redshift ~ 3.

If the metallicity were significantly reduced below local values, then the equivalent hydrogen column density deduced from this observation would be even higher than that discussed here. It may be possible to place a weak lower limit on the metallicity since, if it were reduced to $\lesssim 1\%$ of solar value, the deduced column density would $\gtrsim 10^{24}\mathrm{cm}^{-2}$ and Compton scattering would become important (Kallman & Mushotzky 1985). As we observe more high-redshift quasars, a study of the distribution of intrinsic N_H values at a range of redshifts will give us information on the evolution of the metallicity with redshift.

The existence of an obscured population of quasars with column densities of $\sim 10^{22}\mathrm{cm}^{-2}$ has also been suggested to reconcile the *Einstein* Extended Medium Sensitivity Survey number counts (Gioia *et al.* 1990) with those from *Ginga* fluctuation analysis at higher energies (Warwick & Stewart 1990). Based on our results for PKS0438-436, this obscured population may encompass the whole AGN population rather than only low luminosity objects as originally suggested.

7 References

Brinkmann, W. *et al.* 1992 Proceedings of MPE conference "AGN and the X-ray Background" *in press*

Canizares, C. R. and Kruper, J. 1984 *ApJL* **278**,L99

Canizares, C. R. and White, J. L. 1989 *ApJ* **339**,27

Chokshi, A. 1992 *ApJ submitted*

Gioia, I. M., Maccacaro, T., Schild, R. E., Wolter, A., Stocke, J. T., Morris, S. L. and Henry, J. P. 1990 *ApJS* **72**,567

Halpern, J. P. 1984 *ApJ* **281**,90

Heiles, C. and Cleary, M. N. 1979 *Aust. J. Phys. Suppl.* **47**,1

Heisler, J. and Ostriker, J. P. 1988 *ApJ* **332**,543

Impey, C., D. and Tapia, S. 1988 *ApJ* **333**, 666

Kallman, T. and Krolik, J. 1986 *ApJ* **308**,805

Kallman, T. R. and Mushotzky, R. F. 1985 *ApJ* **292**,49

Kruper, J. S., Urry, C. M. and Canizares, C. R. 1990 *ApJS* **74**,347

Kwan, J. and Krolik, J. H. 1981 *ApJ* **250**,478

Lawrence, A. and Elvis, M. 1982 *ApJ* **256**,410

Madejski, G., *et al.* 1992 Proc. "Frontiers of X-ray Astronomy" ed. K. Koyama, Universal Academic Press *in press*

Madejski, G. M., Mushotzky, R. F., Weaver, K. A., Arnaud, K. A. and Urry, C. M. 1991 *ApJ* **370**, 198

Marscher, A. P. 1988 *ApJ* **334**, 552

Morton, D. C., Savage, A. and Bolton, J. G. 1978 *MNRAS* **185**, 735

Reichert, G. A., Mushotzky, R. F., Petre, R. and Holt, S. S. 1985 *ApJ* **296**, 69

Pan, H. C., Stewart, G. C. and Pounds, K. A. 1990 *MNRAS* **242**, 177

Sanders, D. B., Soifer, T.B., Elias, J. H., Madore, B. F., Matthews, K., Neugebauer, G. and Scoville, N. Z. 1988 *ApJ* **325**, 74

Sargent, W. L. W., Steidel, C. C. and Boksenberg, A. *ApJS* **69**, 703

Shanks, T., Georgantopoulos, I., Stewart, G. C., Pounds, K. A., Boyle, B. J., and Griffiths, R. E., 1991, Nature, **353**, 315

Snowden, S. L. *et al.* 1992 *in preparation*

Warwick, R. S. and Stewart, G. S. 1990 in Proceedings of the 23rd ESLAB Symposium ed.

Nick White [ESA Publications Division], 2,727
Wilkes, B. J. and Elvis, M. 1987 *ApJ* **323**, 243
Wilkes, B. J. Tananbaum, H., Worrall, D. M., Avni, Y., Oey, M. S. and Flanagan, J. 1992 *ApJS in preparation*
Turner, T. J, Weaver, K. A., Mushotzky, R. F., Holt, S. S. and Madejski, G. M. 1991 *ApJ* **381**,85
D.A. Turnshek, A.M. Wolfe, K.M. Lanzetta, F.H. Briggs, R.D. Cohen, C.B. Foltz, H.E. Smith, and B.J. Wilkes, 1989 *Ap.J.*, **344**, 567
Worrall, D. M. and Wilkes, B. J. 1989 *ApJ* **360**,396

Acknowledgements.

This work was carried out with the financial support of grants: NAG5-1724, NAG5-1536, NAGW2201 and has made use of the NASA/IPAC Extragalactic Database (NED) which is operated by the Jet Propulsion Laboratory, California Institute of Technology, under contract with the National Aeronautics and Space Administration

Figure Captions

Figure 1: (a) The best fit for a single power law spectral fit with free local N_H to the spectrum of PKS0438-436. (b) 68%, 90% and 99% confidence contours for the same fit for both PKS0438-436, PKS0439-433. Galactic N_H, $N_H+1\sigma$ are indicated by vertical lines.

Figure 2: a: The confidence contours for a single power law fit assuming Galactic plus intrinsic $N_H$for PKS0438-436. b: The dependence of the deduced equivalent hydrogen column density on the redshift assumed for the absorber.

Table 1: The Quasar Properties.

Name	RA(J2000)	Dec(J2000)	V	z	N_H(Gal)[a] cm−2	ROSAT:Date Time (secs)	Net Counts
PKS0438-436	04 40 17.18	−43 33 09.0	18.8	2.85	1.5±1.0	19-21 Feb 1991	625±28
PKS0439-433	04 41 16.1	−43 13 28	16.4	0.593	"	10725	1028±41

a: Heiles & Cleary 1979

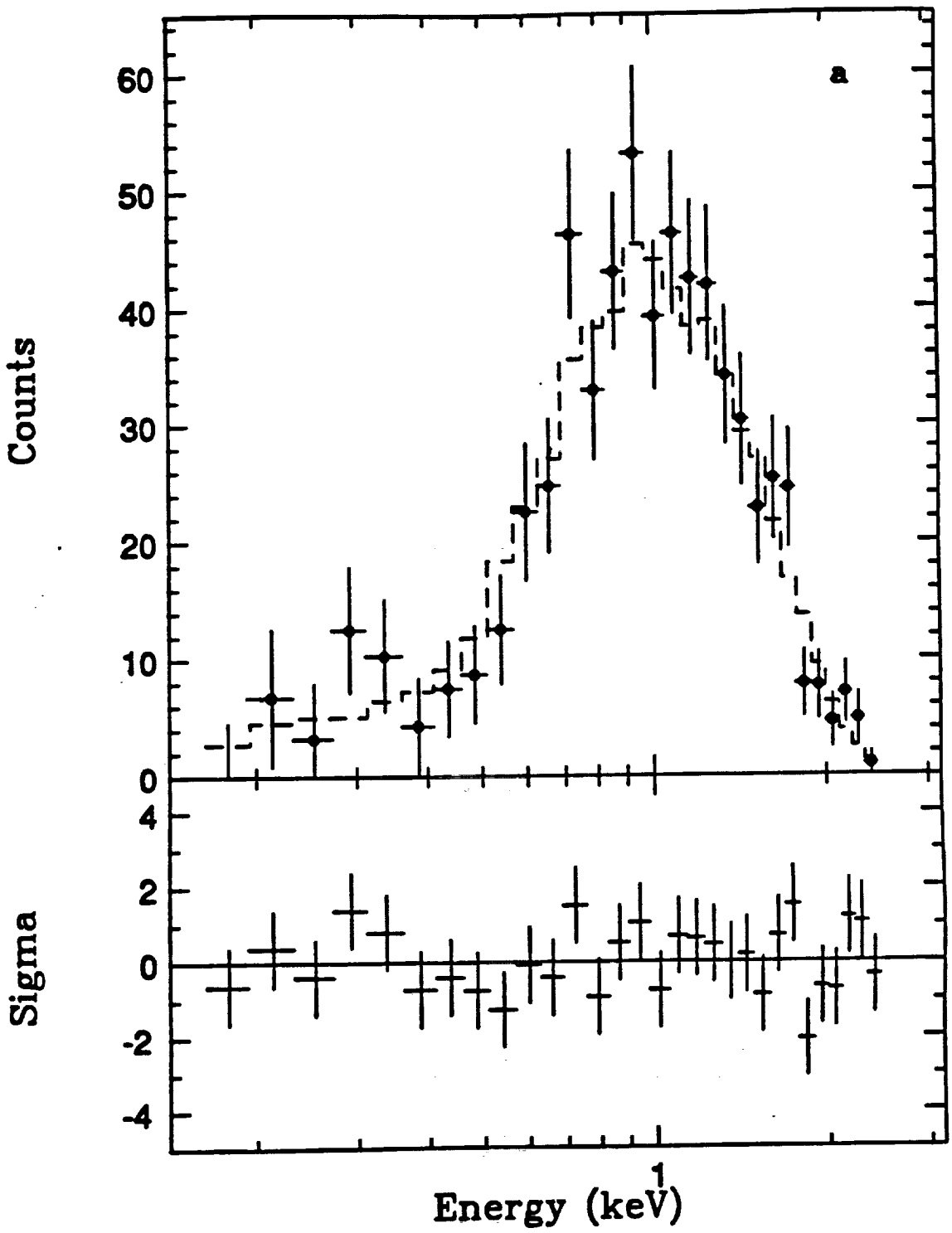

Fig. 1a

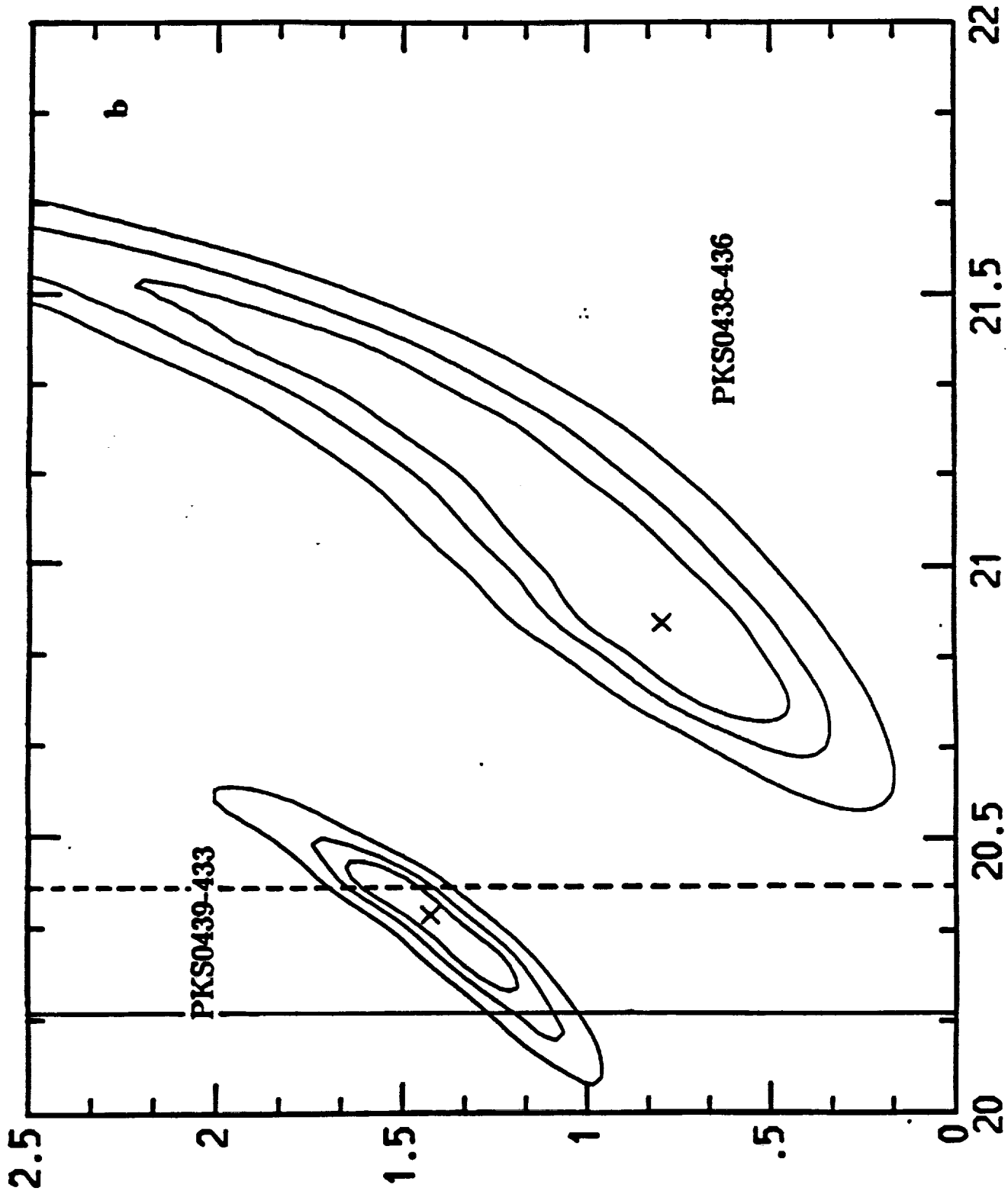
b
PKS0438-436
PKS0439-433
galactic Nh (log)
energy index
20
20.5
21
21.5
22
0
.5
1
1.5
2
2.5

Fig. 1b

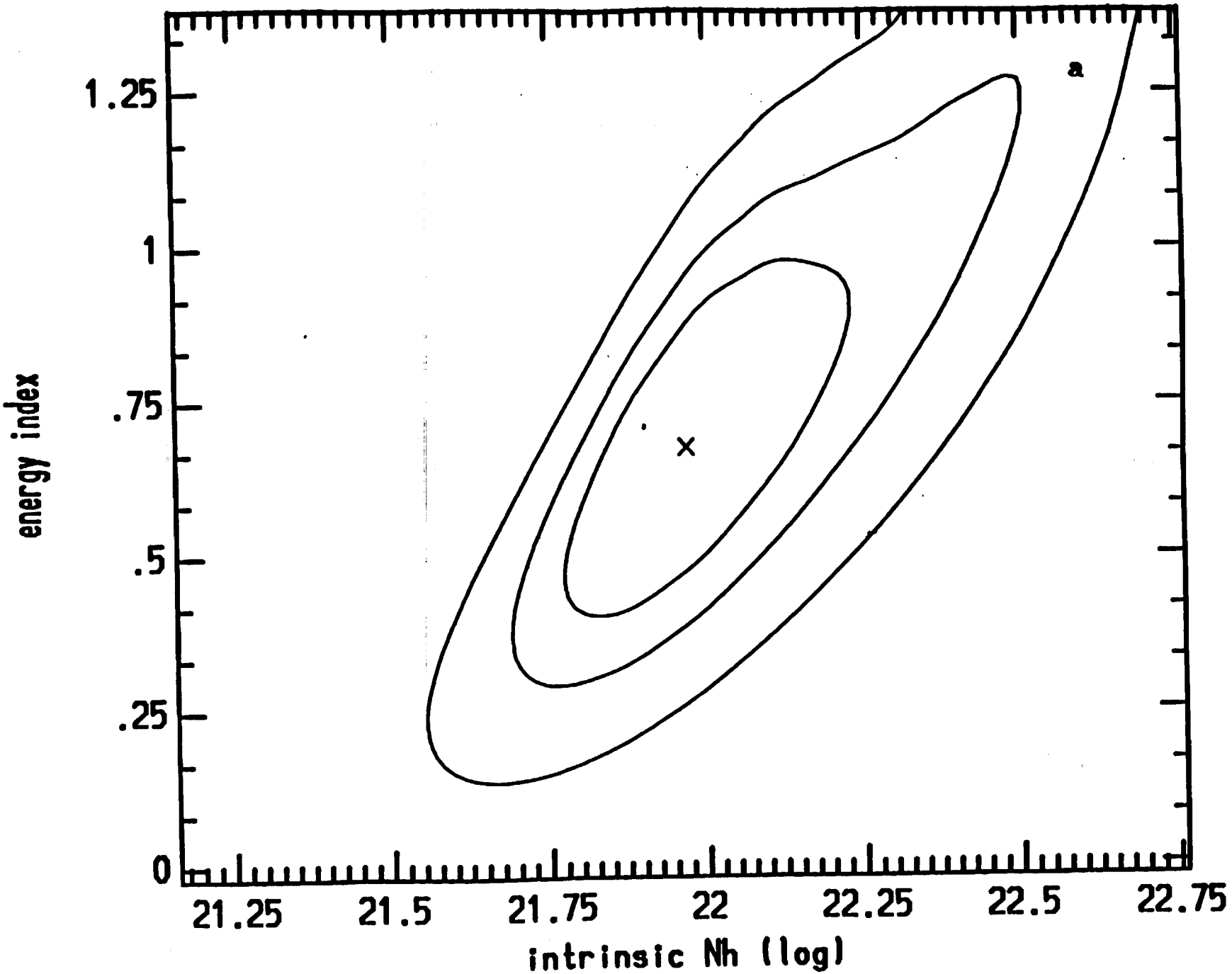
a
1.25
1
.75
.5
.25
0
energy index
21.25
21.5
21.75
22
22.25
22.5
22.75
intrinsic Nh (log)

Fig. 2a

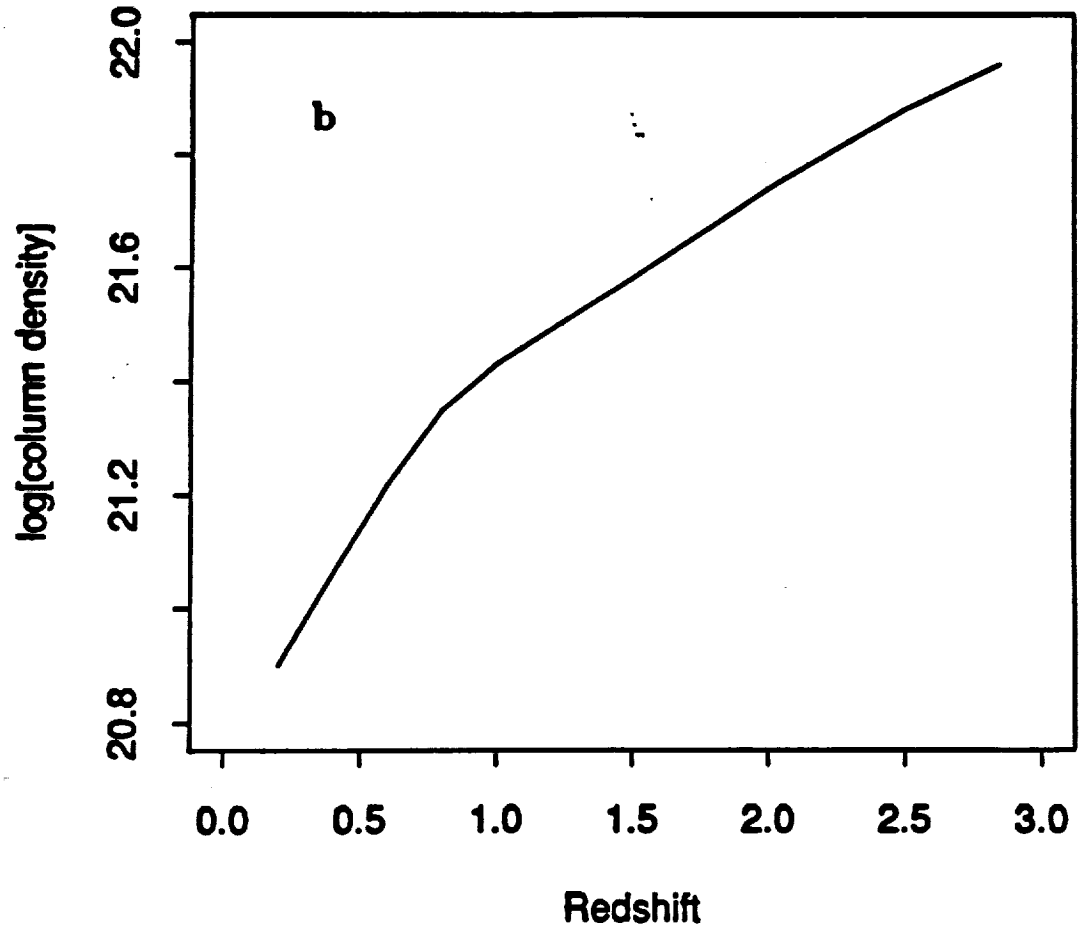
b
log[column density]
22.0
21.6
21.2
20.8
0.0
0.5
1.0
1.5
2.0
2.5
3.0
Redshift

Fig. 2b

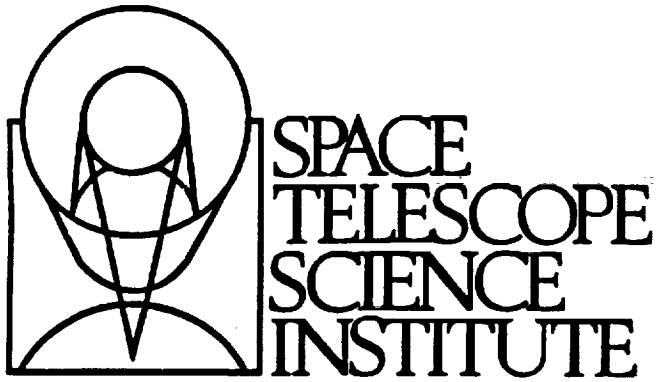

PREPRINT SERIES
No. 635

AN X-RAY IMAGE OF THE SEYFERT GALAXY NGC 1068

A. S. Wilson

M. Elvis

A. Lawrence

J. Bland-Hawthorn

April 1992

Operated by the Association of Universities for Research in Astronomy, Inc., for the National Aeronautics and Space Administration

AN X-RAY IMAGE OF THE SEYFERT GALAXY NGC 1068

A. S. Wilson[1]

Astronomy Department, University of Maryland

College Park, MD 20742

and

Space Telescope Science Institute

3700 San Martin Drive, Baltimore, MD 21218

M. Elvis[1]

Harvard Smithsonian Center for Astrophysics

60 Garden Street, Cambridge, MA 02138

A. Lawrence[1]

Physics Department, Queen Mary and Westfield College

University of London, Mile End Road, London E1 4NS, England

J. Bland-Hawthorn[1]

Department of Space Physics and Astronomy

Rice University, Houston, TX 77251-1892

To be published in the 1 June 1992 issue of the *Astrophysical Journal Letters*

Received 27 January 1992 ; Accepted 18 March 1992

[1]Guest Observer, ROSAT Observatory

ABSTRACT

We present and discuss an image of NGC 1068 with resolution 4″–5″ obtained with the High Resolution Imager on the ROSAT X-ray Observatory in the energy band 0.1–2.4 keV. The map shows a compact nuclear source, circumnuclear extended (diameter $\simeq$ 1.5 kpc) emission, and emission on a scale (diameter $\simeq$ 13 kpc) similar to that of the starburst disk. The circumnuclear emission extends preferentially towards the NE, the same direction as found in several other wavebands. We favor thermal emission from a hot (10^{6-7}K), outflowing wind as the source of the nuclear and circumnuclear emission. This hot gas has a similar pressure to that of the optical line-emitting filaments in the lower density narrow line region, and may be responsible for their confinement. The large scale X-rays are probably dominated by emission from the starburst disk, although a contribution from an extension of the nuclear-driven wind to large radii is possible. The X-ray spectrum of the starburst disk is found to be harder than that of the nucleus. Emission from the starburst, rather than the electron-scattered Seyfert nucleus, may be responsible for much of the hard spectrum emission from NGC 1068 in the 2–10 keV band. Recent modelling of the electron-scattering cone in this galaxy has required the optical depth to photoelectric absorption near 1 keV to be $\leq$1, but this constraint is unnecessary if most of the X-ray emission comes from spatial scales comparable to the starburst and the narrow line region.

1. INTRODUCTION

Studies of spatially extended, soft X-ray emission in active galaxies may yield valuable information about the interaction between the active galactic nucleus (AGN) and its surroundings. Thermal bremsstrahlung emission from hot gas should be ubiquitous, for such gas may be generated in shock waves produced through collisions between high velocity clouds in the narrow line region (NLR), or through entrainment of interstellar clouds in a radio jet, a radio lobe or an outflowing wind. Extended X-ray emission associated with AGN can also result from synchrotron radiation or inverse Compton scattering. X-rays generated by the compact, nuclear X-ray source may be scattered by electrons in the interstellar medium, and be seen as an X-ray "halo".

The nearby (15 Mpc, for H_o = 75 km s^{-1} Mpc^{-1}), luminous ([2-3]$\times 10^{11}$ L$_\odot$) Seyfert galaxy NGC 1068 is an obvious candidate for extended X-ray emission, for it contains high velocity (up to $\simeq$1,000 km s^{-1}) gas clouds in the inner $\simeq$ 15″–20″ (1.1–1.5 kpc; *e.g.*, Cecil, Bland & Tully 1990) and a "linear" radio source, with extent 13″ (950 pc), which is apparently fuelled by collimated ejection from the active nucleus (Wilson & Ulvestad 1982). Further, X-rays should be produced by supernova remnants and X-ray binaries associated with the luminous, 30″ (2.2 kpc) scale, disk "starburst" (*e.g.*, Bruhweiler, Truong & Altner 1991; Telesco *et al.* 1984). Although the spectrum of the *integrated* X-ray emission of NGC 1068 has been measured (Monier & Halpern 1987; Elvis & Lawrence 1988), no studies of its spatial distribution have been published.

A quite different motivation for searching for extended, soft X-ray emission from NGC 1068 is related to the properties of the nuclear, electron scattering zone. Antonucci & Miller (1985) found that the spectrum of NGC 1068 (classically a Seyfert of type 2) in linearly polarized light resembles the spectrum of a Seyfert 1 galaxy. They proposed that the galaxy contains a Seyfert 1 nucleus blocked from direct view by a thick torus, but rendered visible through scattering by a cloud of electrons along the axis of the torus. Miller, Goodrich & Mathews (1991) have inferred an electron temperature of $<3\times10^5$ K for the scattering cloud from limits to broadening of Hβ by the scattering. This low temperature must be reconciled with the high level of ionization implied by the absence of photoelectric absorption in the X-ray spectrum (Elvis & Lawrence 1988) and by the observed energy of the Fe Kα line (Koyama *et al.* 1989). As described in detail by Miller, Goodrich & Mathews (1991), models satisfying these contrasting constraints are possible, but the range allowed for the physical parameters describing the scattering zone is uncomfortably small. The constraints would be eased if some of the X-ray emission originates from larger scales than the scattering zone, and therefore does not have to pass through it.

In order to image NGC 1068 in soft X-rays, we have observed it with the High Resolution Imager (HRI) on the ROSAT X-ray Observatory. The galaxy was observed between July 24 and 26, 1991, for a total integration time ("live time") of 19,947

secs. The image shows obvious extended structure, which is reported here.

2. RESULTS

The spatial resolution of the unsmoothed image can be estimated from a compact X-ray source located 347″ S and 54″ E of the nucleus of NGC 1068. This source contains 218 counts and is probably associated with a ≈15 mag stellar object. An azimuthally averaged, radial profile reveals a FWHM of 4″–5″, and a 50% power radius of $\simeq$ 3.7″, consistent with other HRI observations processed using the current aspect solution (see also Fig. 3).

Contour maps of the X-ray brightness distribution of NGC 1068 are shown in Fig. 1. The data have been smoothed with circular Gaussians of FWHM 1″, 2.5″, and 5″ in Figs. 1a, b, and c, respectively. While residual errors in the aspect solution render fine scale (a few arc secs) details uncertain, Fig. 1a reveals a compact source within 3″ of the optical nucleus (Clements 1981), plus emission extending asymmetrically to the N and NE. The highest resolution map suggests the presence of localised "ridges" at 6″–12″ from the nucleus towards the NE (p.a. $\simeq$ 10°–35°). At larger distances (15″–60″) from the nucleus, fainter X-ray emission is found aligned along p.a. 35°–45° to both NE and SW of the nucleus (Fig. 1c). The ROSAT HRI has some energy resolution, and the pulse height distributions for the nuclear emission, the circumnuclear emission, and the very extended emission are all *inconsistent* with that found for signals dominated by uv contamination (as appears to be the case for an HRI observation of Vega [Zombeck, private communication]).

Extensions from the nucleus of NGC 1068 towards the N and NE are seen on the arc sec or sub arc sec scale in several other wavebands, including radio continuum (Ulvestad, Neff & Wilson 1987), mid-infrared (Tresch-Fienberg *et al.* 1987), optical emission line (Pogge 1989; Evans *et al.* 1991), and optical continuum (Balick & Heckman 1985; Lynds *et al.* 1991). The axis (p.a. 35°–45°) of the larger scale X-ray emission (Fig. 1c) may be compared with the major axis (p.a. 50°–55°) of the ovally distorted disk on the 40″ (diameter) scale (Baldwin, Wilson, & Whittle 1987), and the direction (p.a. 48°) of the 36″ length stellar bar seen at 2 μm (Scoville *et al.* 1988). Fig. 2 (Plate) shows the low resolution image superimposed on a blue band photograph. It can be seen that the outer X-ray contours follow the edge of the brightest part of the visible disk quite well, and there are suggestions of associations between details of the emission in the two wavebands. The overall similarity of this faint, outer X-ray emission to the optical image suggests that it is associated with the "starburst" disk, and presumably represents emission from supernova remnants, X-ray binaries, and possibly a starburst-driven wind. We prefer this interpretation over the alternative, which would explain this outer emission in terms of a large scale wind driven by the Seyfert nucleus (see Section 3.1).

An azimuthally averaged radial profile is shown in Fig 3. The data suggest faint emission to a radius of $\simeq$1.5′, although the reality of the outermost emission must be considered uncertain until improved calibrations of the HRI are available. In order to estimate the fraction of the emission which is extended, a point spread function (Fig. 3) was first obtained from three calibration sources. This point spread function was then scaled to the peak flux at the nucleus of NGC 1068 and subtracted from it. The result is that 45±5% of the total detected HRI flux is spatially extended.

Within a radius of 100″ from the nucleus, the total count rate is 0.57 counts s^{-1} (after background subtraction). If we adopt the spectral parameters obtained by Monier & Halpern (1987) from Einstein IPC observations, namely an intrinsic (unabsorbed) flux of 5.8×10^{-11} erg cm^{-2} s^{-1} in the ROSAT band (0.1–2.4 keV), a power law spectrum of energy index $\alpha_E = 2.0$ (so $F_E \simeq 2.5\times10^{-29}(E/keV)^{-2}$ erg cm^{-2} s^{-1} Hz^{-1}), and a hydrogen column N_h = (3–5)$\times10^{20}$ cm^{-2}, a total ROSAT HRI count rate of 0.56–0.36 counts s^{-1} is predicted. The good agreement between the first of these predicted count rates and that observed with ROSAT confirms that the hydrogen column density is close to the Galactic value of $N_h = 3.0\times10^{20}$ cm^{-2} (Elvis & Lawrence 1988).

It is clear that the spectrum of the nuclear source is much softer than that of the very extended emission more than 10″ from the nucleus (Fig. 3). At this early stage in the ROSAT pointed phase, no good calibration of the HRI energy response has been made, so a full investigation of the spectral characteristics of the different components in NGC 1068 must be deferred to a later paper. Nevertheless, the steep spectrum emission seen with the Einstein IPC (Monier & Halpern 1987) must originate in the nucleus and possibly also the circumnuclear region. In the following Section, we argue that the hard component (with $F_E \propto E^{-0.5}$) detected from NGC 1068 in the 2–10 keV band(Elvis & Lawrence 1988; Koyama *et al.* 1989) may be dominated by emission from the extended starburst, rather than the Seyfert nucleus as has usually been assumed.

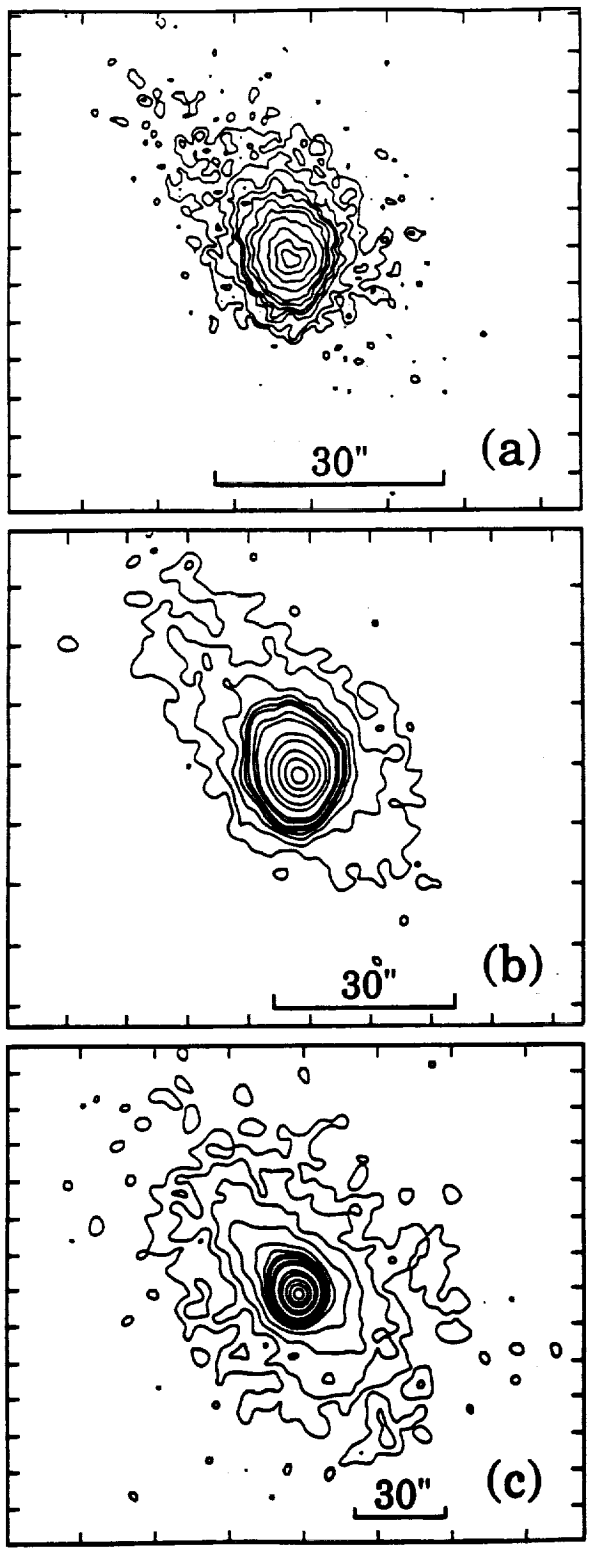

Figure 1—Contour maps of the distribution of X-ray emission in NGC 1068. N is up and E to the left. In order to show the X-ray emission on different spatial scales, the data have been smoothed with different Gaussian functions in the three panels. The peak brightnesses listed are for the ROSAT HRI band *before* photoelectric absorption, assuming a power law spectrum of index $\alpha_E = 2.0$ and a hydrogen column $N_h = 3\times10^{20}$ cm^{-2}. (a) Smoothing function is 1″ (FWHM). Contours are plotted at 1.25, 2.5, 5, 7.5, 10, 15, 20, 30, 50, 70 and 90% of the peak brightness of 37.9 counts pixel^{-1} (1 pixel = 0.5″×0.5″) or 7.7×10^{-13} erg cm^{-2} s^{-1} (arc sec)$^{-2}$. (b) Smoothing function is 2.5″ (FWHM). Contours are plotted at 0.5, 1, 2, 3, 4, 5, 7.5, 10, 20, 30, 50, 70, and 90% of the peak brightness of 32.3 counts pixel^{-1} or 6.6×10^{-13} erg cm^{-2} s^{-1} (arc sec)$^{-2}$. (c) Smoothing function is 5″ (FWHM). Contours are plotted at 0.125, 0.25, 0.5, 1, 2, 3, 4, 5, 7.5, 10, 20, 30, 50, 70, and 90% of the peak brightness of 23.2 counts pixel^{-1} or 4.7×10^{-13} erg cm^{-2} s^{-1} (arc sec)$^{-2}$.

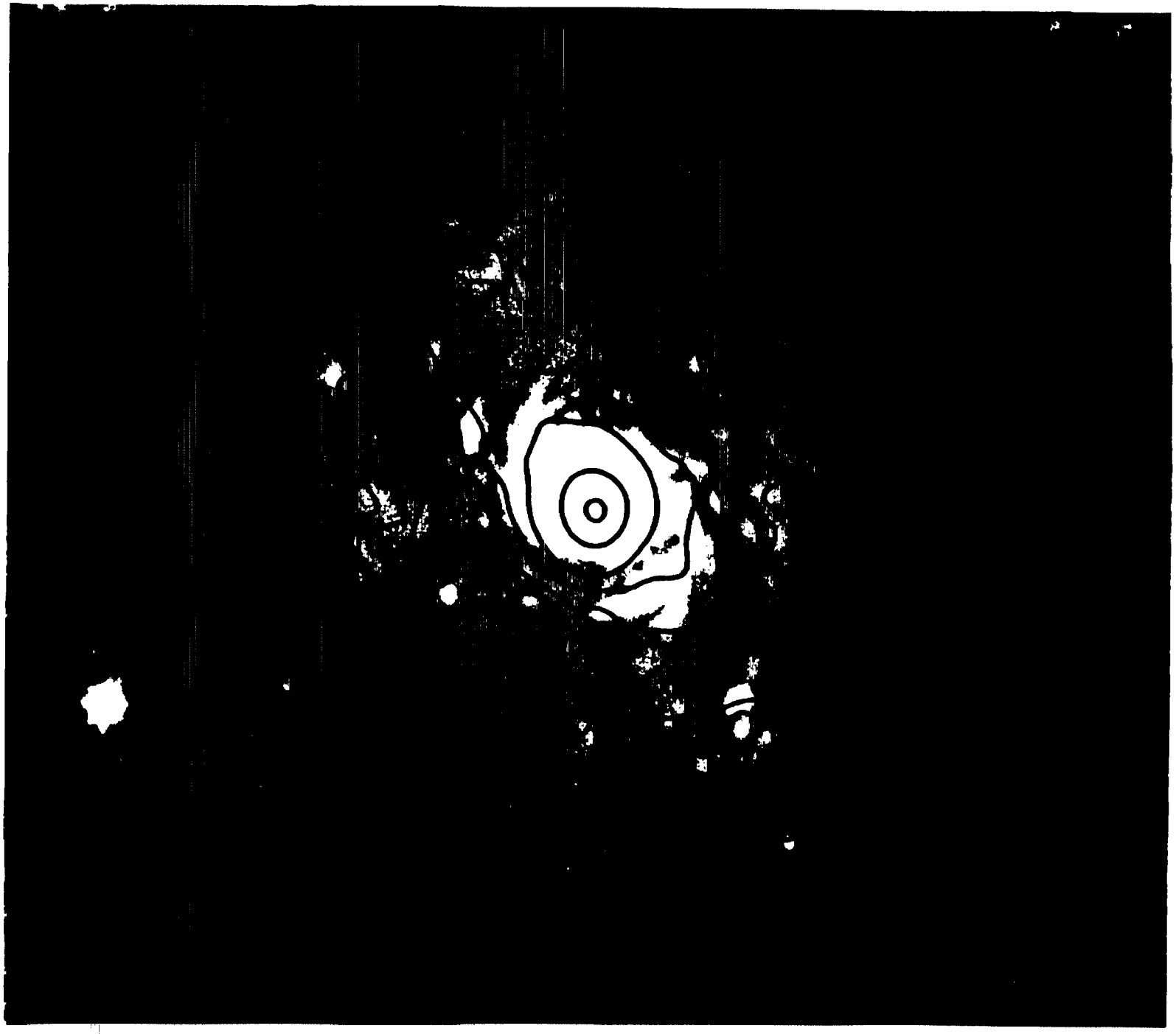

Figure 2, Plate—Contour map of the X-ray data (smoothed with a 5″ FWHM Gaussian function) superimposed on a blue (IIaO emulsion) print from the Hubble atlas (Sandage 1961). N is up and E to the left. Contours are plotted at 0.125, 0.25, 0.5, 1, 3, 30, and 90% of the peak brightness. The tick marks along the horizontal and vertical axes are separated by 25″ and 12.5″ respectively (the field size is 3.23′ E-W × 2.82′ N-S).

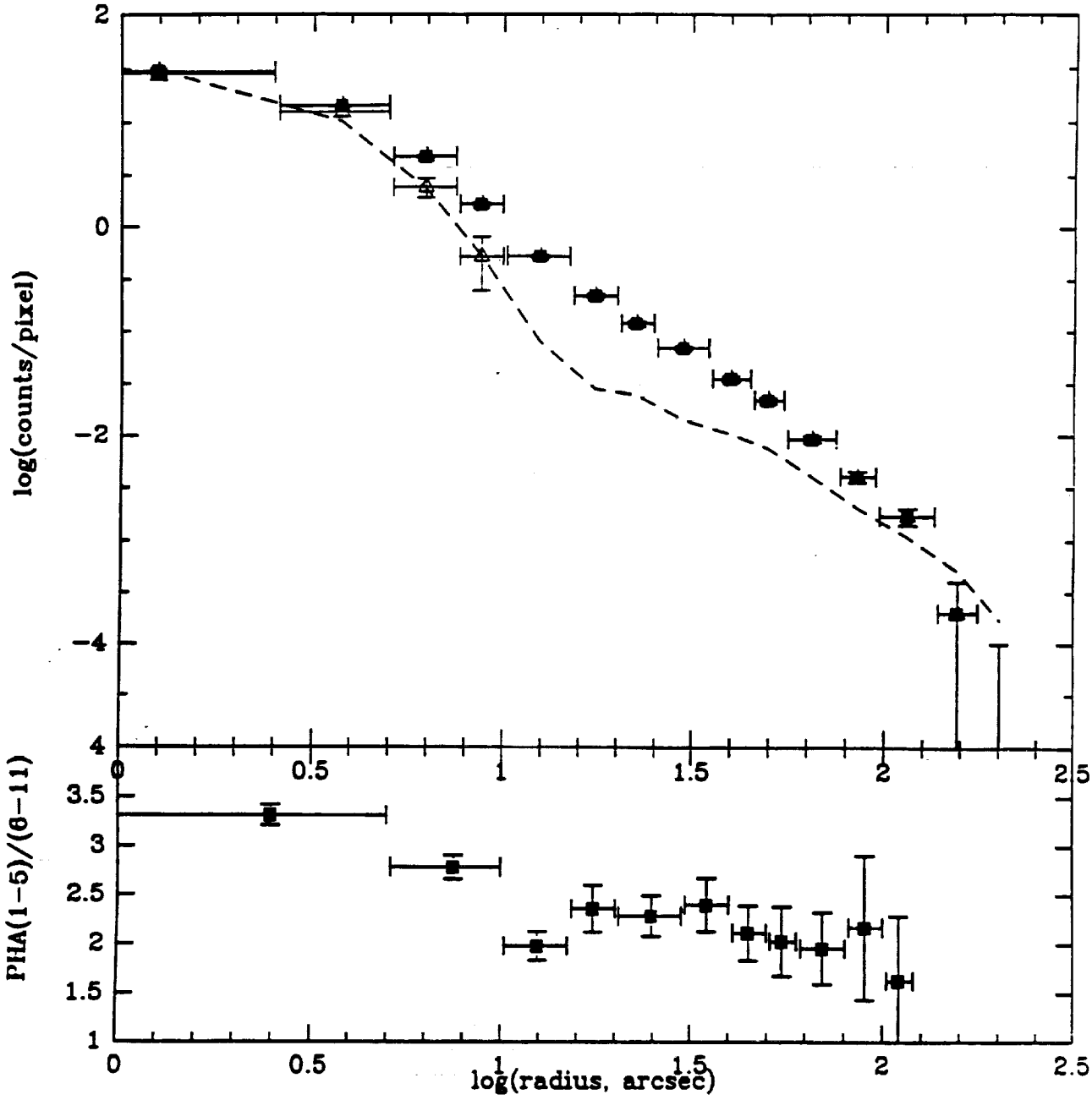

Figure 3—The top panel shows the log of the azimuthally averaged number of counts per pixel for NGC 1068 (filled symbols), the star 6′ to the S of NGC 1068 (open triangles), and the point spread function derived from the average of the calibration sources LMCX-1, HZ43 and ARLac (dashed line) plotted against log radius (distance from peak flux). The lower panel is a plot of the "softness ratio" (counts in pha channels 1–5 divided by counts in pha channels 6–11) for NGC 1068 versus log radius. This ratio is seen to decrease (*i.e.*, the spectrum hardens) with increasing radius.

3. DISCUSSION

Our observations show that the soft X-ray emission of NGC 1068 comprises an unresolved source associated with the Seyfert nucleus, emission extending from the nucleus on the several arc second scale, and large-scale emission reaching $\simeq$1.5′ (6.6 kpc) from the nucleus. Broad optical emission lines are detected out to the inner edge of the molecular ring, some 10″ (730 pc) from the nucleus (Baldwin, Wilson & Whittle 1987), and delineate the extent of the kinematic influence of the nuclear activity. The brightest X-ray emission is also contained within $\simeq$10″ of the Seyfert nucleus. The large-scale emission correlates quite well with the starburst disk (Fig. 2 [Plate]), although some of this X-ray emission could be fuelled by the nucleus (*e.g.*, as a large scale wind), given its rough alignment with the nuclear elongation. Of the total count rate, some 55% (3.2×10^{-11} erg cm^{-2} s^{-1} before photoelectric absorption and assuming a power law spectrum with $\alpha_E = 2.0$) then represents *unresolved* nuclear emission, $\simeq$23% (1.3×10^{-11} erg cm^{-2} s^{-1}) is *extended* nuclear emission, and the remaining 22% (1.3×10^{-11} erg cm^{-2} s^{-1} for the above power law spectrum, or 5.7×10^{-12} erg cm^{-2} s^{-1} for thermal bremsstrahlung emission with kT = 5 keV) originates in the starburst disk. The corresponding X-ray luminosities are 8×10^{41}, 3×10^{41}, and $(3\text{–}1.4)\times10^{41}$ erg s^{-1}, respectively. Although the quantitative separation between nucleus and starburst disk is somewhat arbitrary, it seems clear that both contribute to the X-ray emission, so in the following discussion we consider the likely emission processes separately.

3.1 The X-ray Emission of the Nucleus

The unresolved and extended nuclear X-rays could result from synchrotron radiation, inverse Compton scattering, thermal emission processes or electron scattering of an unresolved nuclear source. We discuss each of these possibilities in turn.

(i) Synchrotron Radiation

Synchrotron radiation in the ROSAT band would require relativistic electrons with $\gamma \simeq 10^7$ given the equipartition magnetic fields of 10^{-4}–10^{-3} gauss in the radio core and lobes (*e.g.*, Wilson & Ulvestad 1987). The synchrotron half lives would be only $\simeq$1–10 yrs. The half lives of these electrons to inverse Compton scattering can be even shorter in regions close to the nucleus where the energy density in mid-infrared photons is larger than that of the magnetic field. For these reasons, we consider a synchrotron model implausible.

(ii) Inverse Compton Radiation

The observed photon energy density close to the nucleus of NGC 1068 is dominated by radiation with wavelengths near 20μm (Telesco *et al.* 1984). Upward scattering of these photons to $\simeq$1 keV requires relativistic electrons with $\gamma \simeq 100$. Such electrons would radiate synchrotron radiation at frequencies of MHz to tens of MHz. The total radio power emitted in the 1–100 MHz band is only $\simeq1\times10^{39}$ erg s^{-1}, a factor of 1,000 below the observed nuclear emission in the ROSAT band. Thus, a viable inverse Compton model would require these electrons to lose energy primarily to the radiation field. If the relativistic electrons are confined to the observed radio features, the magnetic field needs to be well below equipartition. Alternatively, a large population of relativistic electrons outside the radio features, where the field could be very weak, would be required.

(iii) Thermal Emission

A more promising model for the extended, nuclear X-rays is thermal emission from hot gas in a nucleus-driven wind. Assuming the gas is in collisional equilibrium at a temperature of 10^6–10^7 K and that the X-rays extend to 10″ (730 pc) from the nucleus, a density (assumed uniform) of 2.2–0.9 cm^{-3} is required to account for the X-ray luminosity (Raymond & Smith 1977). The mass of hot gas is $(9\text{–}4)\times10^7 M_\odot$ in this model, but would be less if the gas is clumped. The pressure of this hot component would be $\simeq(3\text{–}12)\times10^{-10}$ erg cm^{-3}. This value is comparable to that required to confine the optical line-emitting filaments in the lower density region (Shields & Oke 1975), for which the density, temperature and pressure are $\simeq$800 cm^{-3}, $\simeq10^4$ K and $(7\text{–}11)\times10^{-10}$ erg cm^{-3}, respectively. This result supports models in which the cool, optical line-emitting filaments condense out of, or are entrained by, a hot, outflowing wind (*e.g.*, Krolik & Vrtilek 1984).

(iv) Electron-Scattered Nuclear Radiation

Elvis *et al.* (1990) have argued against electron-scattered nuclear radiation as the source of the *spatially extended*, soft X-ray emission detected from several Seyfert galaxies. They noted that the extended gas must be sufficiently highly ionized that it does not absorb the X-rays. If this is achieved thermally, a temperature above $\simeq3\times10^6$ K is needed, and direct bremsstrahlung then dominates over scattered radiation. If it is achieved radiatively, the ionization parameter of the gas at distances of 0.3–1 kpc from the nucleus must be so high that the luminos-

ity of the central source becomes much larger than is observed. Application of this argument to the circumnuclear X-ray emission of NGC 1068 gives a required central luminosity of $\geq 2\times10^{46}$ erg s^{-1}. This number is more than an order of magnitude above the observed bolometric luminosity of the nucleus of NGC 1068, rendering implausible an electron scattering model for the *extended* nuclear emission.

3.2 The X-ray Emission of the Starburst

Fabbiano & Trinchieri (1985) have found an approximately linear correlation between X-ray and blue luminosities for the disks of spiral galaxies, and concluded that the X-ray emission of spirals is largely connected with the Population I component. It is then of interest to see whether the starburst disk of NGC 1068 conforms with this relation. Adopting $B_T^0 = 9.17$ (de Vaucouleurs, de Vaucouleurs & Corwin 1976) and subtracting off the nuclear contribution, we find $f_B = 8.2\times10^{-24}$ erg cm^{-2} s^{-1} Hz^{-1} for the disk alone. Assuming the disk emission is thermal with a temperature kT = 5 keV, $f_{2keV} = 7.1\times10^{-30}$ erg cm^{-2} s^{-1} Hz^{-1}, so $f_{2keV}/f_B = 8.7\times10^{-7}$. This ratio is larger than is typical of normal spirals, for which the distribution of f_{2keV}/f_B peaks near $\simeq1.6\times10^{-7}$ (Fabbiano & Trinchieri 1985), but is two to three orders of magnitude lower than that for type 1 Seyferts. The ratio for the disk of NGC 1068 is, however, similar to those found for peculiar galaxies experiencing bursts of star formation (Fabbiano, Feigelson, & Zamorani 1982). A further comparison may be made with the results of Griffiths and Padovani (1990), who showed that the average of the X-ray to far-infrared luminosity ratio log L(0.5–3.0 keV)/L(60 μm) = -3.32 ± 0.10 for IRAS galaxies and = -3.27 ± 0.11 for starburst/interacting galaxies. For the disk of NGC 1068, this ratio is -3.27. These similarities with galaxies undergoing active star formation are consistent with our conclusion that the very extended X-ray emission of NGC 1068 is associated with the starburst disk.

By extrapolating our measured flux to higher energies, the flux of the starburst disk in the 2–10 keV band is predicted to be 2.5×10^{-12}, 5.8×10^{-12} and 8.4×10^{-12} erg cm^{-2} s^{-1} for a 2 keV (the minimum temperature of a spiral galaxy disk in the 0.5–3.0 keV band [Fabbiano & Trinchieri 1987]) thermal spectrum, a 5 keV thermal spectrum, and an α_E = 0.5 power law spectrum, respectively. These numbers may be compared with the measured fluxes of F(2–10 keV) = 6.1×10^{-12} (Elvis & Lawrence 1988), 5.0×10^{-12} (Koyama *et al.* 1989), and 3.4×10^{-12} erg cm^{-2} s^{-1} (K. A. Weaver, private communication, from a BBXRT observation). The observed spectrum of the 2–10 keV emission can be represented by a power law with $\alpha_E = 0.5\pm0.05$ or thermal emission with kT > 27 keV (Koyama *et al.* 1989). The emission from the starburst *overpredicts* the observed 2–10 keV flux for these spectral parameters. *Thus emission from the starburst may account for most or all of the hard spectrum emission seen in 2–10 keV band.* An alternative interpretation, which cannot be ruled out at present, is that the apparent hard spectrum of the very extended emission in the ROSAT band results from strong Fe L line emission near 1 keV. In any case, it is likely that some part of the FeFe K line emission seen from NGC 1068 (Koyama *et al.* 1989) originates from X-ray binaries in the starburst. A contribution from the blocked Seyfert nucleus is also probably present, for the total observed Fe K equivalent width of 2.9 keV (Marshall *et al.* 1991) is much larger than can be expected from an ensemble of X-ray binaries.

In constraining their models of the nuclear scattering cone, Miller, Goodrich & Mathews (1991) required the optical depth to photoelectric absorption through this region $\tau(1\ \mathrm{keV}) \leq 1$. However, we have argued that most of the hard spectrum emission near this energy is probably from the starburst. Further, the steep spectrum, soft emission from the nucleus is partially resolved in our image, so much of this component may come from outside the electron scattering zone. Therefore, it is no longer necessary to demand that the scattering cone in NGC 1068 be optically thin to photoelectric absorption below a few keV. The removal of this observational constraint permits a greater range of model parameters for this region (see Miller, Goodrich and Mathews' Table 4).

4. CONCLUSIONS

The chief conclusions of this paper are as follows:

(i) An X-ray map of NGC 1068 reveals an unresolved nuclear source, extended ($\simeq$ 1.5 kpc) emission around the nucleus, and extended ($\simeq$ 13 kpc) emission from the starburst disk. Since spatially extended, soft X-ray emission is now known in several other Seyfert galaxies (Elvis *et al.* 1990), their integrated soft X-ray spectra *cannot* be directly interpreted in terms of emission processes near the black hole or accretion disk unless time variability is observed.

(ii) The extended circumnuclear emission aligns towards the NE, the same direction as found for

the resolved emission of the active nucleus in several other wavebands.

(iii) While it is hard to rule out synchrotron radiation, inverse Compton scattering and electron-scattered nuclear radiation, we prefer thermal emission from a hot wind as the source of the steep-spectrum, nuclear and circumnuclear emission. The thermal pressure of this hot gas is similar to that of the low density component of the narrow-line region, suggesting confinement of the narrow line clouds in the hot wind.

(iv) The disk of NGC 1068 has ratios of soft X-ray to B band and soft X-ray to 60 μm luminosities which are similar to those found for other starburst systems.

(v) The X-ray spectrum of the starburst disk is harder than that of the nuclear emission. By adopting a plausible spectrum and extrapolating our measured flux, we find that the starburst disk may well contribute most of the hard component seen in the 2–10 keV band. This result is contrary to the current prevailing opinion that this hard component originates through electron scattering of a source in the Seyfert nucleus. Some contribution from such a source may, however, still be present.

(vi) In view of point (v), it is no longer clear that the nuclear electron scattering cone in NGC 1068 must be optically thin to photoelectric absorption near 1 keV. Because most of the steep spectrum, soft (0.1–3 keV) nuclear X-rays could also come from outside the scattering cone, there is no compelling reason to believe that this region is optically thin to photoelectric absorption at *any* energy below a few keV.

Acknowledgements

We are grateful to Larry David, Gail A. Reichert, Eric M. Schlegel, T. Jane Turner and Martin Zombeck for assistance with the data analysis, and to Pepi Fabbiano, Richard E. Griffiths, Tim M. Heckman, Julian H. Krolik, and Jean H. Swank for discussions. This research was supported by NASA grants NAG5-1532 and NAGW-2689 to the University of Maryland, and NAG5-1536 to SAO.

REFERENCES

Antonucci, R. R. J., & Miller, J. S. 1985, ApJ, 297, 621

Baldwin, J. E., Wilson, A. S., & Whittle, M. 1987, ApJ, 319, 84

Balick, B., & Heckman, T. M. 1985, AJ, 90, 197

Bruhweiler, F. C., Truong, K. Q., & Altner, B. 1991, ApJ, 379, 596

Cecil, G., Bland, J., & Tully, R. B. 1990, ApJ, 355, 70

Clements, E. D. 1981, MNRAS, 197, 829

de Vaucouleurs, G., de Vaucouleurs, A., & Corwin, H. G. 1976, *Second Reference Catalogue of Bright Galaxies*, (Austin: University of Texas Press)

Elvis, M., & Lawrence, A. 1988, ApJ, 331, 161

Elvis, M., Fassnacht, C., Wilson, A. S., & Briel, U. 1990, ApJ, 361, 459

Evans, I. N., Ford, H. C., Kinney, A. L., Antonucci, R. R. J., Armus, L., & Caganoff, S. 1991, ApJ, 369, L27

Fabbiano, G., Feigelson, E., & Zamorani, G. 1982, ApJ, 256, 397

Fabbiano, G., & Trinchieri, G. 1985, ApJ, 296, 430

Fabbiano, G., & Trinchieri, G. 1987, ApJ, 315, 46

Griffiths, R. E., & Padovani, P. 1990, ApJ, 360, 483

Koyama, K., Inoue, H., Tanaka, Y., Awaki, H., Takano, S., Ohashi, T., & Matsuoka, M. 1989, PASJ, 41, 731

Krolik, J. H., & Vrtilek, J. M. 1984, ApJ, 279, 521

Lynds, R., *et al.* 1991, ApJ, 369, L31

Marshall, F. E. *et al.* 1991, To be published in the Proceedings of the 28th Yamada Conference *Frontiers of X-ray Astronomy*

Miller, J. S., Goodrich, R. W., & Mathews, W. G. 1991, ApJ, 378, 47

Monier, R., & Halpern, J. P. 1987, ApJ, 315, L17

Pogge, R. W. 1989, ApJ, 345, 730

Raymond, J. C., & Smith, B. W. 1977, ApJS, 35, 419

Sandage, Allan 1961, *The Hubble Atlas of Galaxies*, (Carnegie Institution of Washington: Washington D. C.)

Scoville, N. Z., Matthews, K., Carico, D. P., & Sanders, D. B. 1988, ApJ, 327, L61

Shields, G. A., & Oke, J. B. 1975, ApJ, 197, 5

Telesco, C. M., Becklin, E. E., Wynn-Williams, C. G., & Harper, D. A. 1984, ApJ, 282, 427

Tresch-Fienberg, R., Fazio, G. G., Gezari, D. Y., Hoffmann, W. F., Lamb, G. M., Shu, P. K., & McCreight, C. R. 1987, ApJ, 312, 542

Ulvestad, J. S., Neff, S. G., & Wilson, A. S. 1987, AJ, 93, 22

Wilson, A. S., & Ulvestad, J. S. 1982, ApJ, 263, 576

Wilson, A. S., & Ulvestad, J. S. 1987, ApJ, 319, 105

Quasar X-ray Spectra Revisited

P. Shastri[1], B.J. Wilkes[2], M. Elvis[2] and J. McDowell[2]

May 2, 1992
ApJ. Submitted

1: Department of Astronomy, University of Texas, Austin
2: Harvard-Smithsonian Center for Astrophysics, Cambridge

1 Abstract

A sample of 45 quasars observed by the IPC on the *Einstein* satellite is used to re-examine the relationship between the soft (0.2-3.5 keV) X-ray energy index and radio-loudness. We find that, (1) the tendency for radio-loud quasars to have systematically flatter X-ray slopes than radio-quiet quasars is confirmed with the soft X-ray excess having negligible effect; (2) there is a tendency for the flatness of the X-ray slope to correlate with radio core-dominance for radio-loud quasars, suggesting that a component of the X-ray emission is relativistically beamed; (3) for the RQQs the soft X-ray slopes, with a mean of ~ 1.0, are consistent with the slopes found at higher energies (2-10 keV) although steeper than those observed for Seyfert 1 galaxies (also 2-10 keV) where the reflection model gives a good fit to the data; (4) the correlation of FeII emission line strength with X-ray energy index is confirmed for radio-quiet quasars using a subset of 18 quasars. The radio-loud quasars show no evidence for a correlation. This relation suggests a connection between the ionizing continuum and the line emission from the broad emission line region (BELR) of radio-quiet quasars, but in the opposite sense to that predicted by current photoionization models; (5) the correlations of X-ray slope with radio core dominance and FeII equivalent width within the radio-loud and radio-quiet sub-classes respectively imply that the observed wide range of X-ray spectral slopes is real rather than due to the large measuring uncertainties for individual objects.

2 Introduction

The powerful X-ray emission that is commonly seen from quasars and other active galactic nuclei is widely believed to originate close to the "central engine" in these objects. Recent studies have made it clear that there is a wide range in the energy indices of the X-ray emission, both in the soft ($\sim$0.3-2keV: Wilkes and Elvis 1987) and hard (2-10keV: Comastri *et al.* 1992; Williams *et al.* 1992) energy ranges, laying to rest the older view that X-ray slopes of all broad-line active galactic nuclei can be adequately described by a single

power law of energy slope ~0.7 (*e.g.* Mushotzky 1984). The details of the X-ray emission mechanisms in different types of quasars, however, are not well understood.

Wilkes and Elvis (1987) derived X-ray energy indices, $\alpha_E (f_\nu \sim \nu^{-\alpha_E})$, in the soft X-ray region (0.2-3.5 keV) for a sample of 33 quasars that were observed with sufficient signal-to-noise with the *Einstein* IPC. They reported that the best-fit power-law energy slopes have a wide range (−0.2 to 1.8), and that radio-loudness correlated with the soft X-ray energy index in the sense that radio-loud quasars (RLQs) had flatter X-ray slopes than radio-quiet quasars (RQQs). They argued for a two-component model for the X-ray emission: one linked to the radio-emission and of somewhat flatter slope (~0.5); and the second of steeper slope (~1) that was ubiquitous in quasars. Wilkes and Elvis (1987) explain the difference between these soft slopes and the mean slope of ~0.7 observed at higher energies in terms of a mixing of the two components. They also found evidence for an upturn in the X-ray spectrum at lower energies (<0.3keV) - the "ultrasoft excess" - as discovered by EXOSAT (Arnaud *et al.* 1985).

Here we study the behavior of the X-ray energy indices of quasars with an enlarged sample of 45 objects using new IPC spectral fits from the atlas of quasar energy distributions (Elvis *et al.* 1992). When required by the ultra-soft excess, we use updated X-ray slopes from Masnou *et al.* (1992), which have been determined with a broken power-law which properly accounts for this excess. We re-examine the connection with radio-loudness (Wilkes and Elvis 1987) and with the radio core-dominance parameter (Shastri 1991), and also consider a possible relation between X-ray slope and the strength of the FeII(optical) emission lines suggested by Wilkes, Elvis and McHardy (1987) but later questioned by Boroson (1989) and Zheng and O'Brien (1990).

3 Radio-loud and radio-quiet quasars

Here we define radio-loudness (R_{L_t}) as $\log(f_R/f_B)$, where f_R and f_B are the flux densities (in mJy) in the 5GHz and B bands respectively. f_B is calculated from the B magnitude using $m_B(0) = 4440$Jy (Johnson 1966). When B magnitudes were not available V magnitudes were used. Note that this definition differs from the one adopted by Wilkes and Elvis (1987) who took f_R to be the core radio flux density where available rather than the total value. Here we use the radio-loudness parameter (R_{L_t}) to distinguish between quasars that do exhibit the phenomenon of powerful radio jets and those that do not. This change largely affects the values for RLQs. In Fig. 1a we show the distribution of radio-loudness for the quasars in our sample. The distribution is clearly bimodal. A quasar is thus classified as "radio-loud" when $\log(f_R/f_B) > 2$.

In Tables 1 and 2, the updated soft X-ray energy indices are listed for the RQQs and RLQs respectively. The distributions of the X-ray energy indices are shown in Fig. 1b. The RLQs have stochastically flatter X-ray spectral slopes than the RQQs at a level >99.95% as given by a Mann-Whitney U test. This confirms the earlier result of Wilkes and Elvis (1987). The RQQ 1803+676 remains an exceptional object with an extremely flat ($\simeq -0.2$) slope.

A simple mean of the X-ray slopes for the RQQs is 1.0 ± 0.1, in good agreement with the mostly overlapping sample of Wilkes and Elvis (1987), and with the higher energy (2-10

keV) slopes determined from EXOSAT and *Ginga* for a similar sample of quasars (Comastri *et al.* 1992; Williams *et al.* 1992). A weighted mean is somewhat lower, 0.85±0.02, due to the strong dominance of a small number of objects with well-determined slopes. Notably, the quasar slopes are systematically steeper than the high energy slopes seen in Seyfert 1 galaxies where reflection of X-rays from cool, optically thick gas gives a good fit to the data (Pounds *et al.* 1990, Williams *et al.* 1992).

In Fig. 2 the radio-loudness parameter (R_{L_t}) is plotted against the soft X-ray energy index. The systematic difference between RLQs and RQQs reported by Wilkes and Elvis (1987) is once again clear (see also Fig 1b). The formal significance of a correlation between α_E and R_{L_t} is >99.5%) although the distribution of the data suggests two classes of objects rather than a real correlation. There is no significant correlation within the sub-samples of RQQs or RLQs (<90% probability, Spearman Rank test), supporting the idea that they form two different populations (Peacock, Miller and Mead, 1986; Smith and Heckman 1990; Williams *et al.* 1992). The dichotomy is consistent with the suggestion that differing emission mechanisms dominate the X-ray emission in the two classes, as originally suggested by Zamorani *et al.* (1981).

4 X-ray slopes and radio-core dominance

In the framework of the "unified interpretation" for RLQs (Blandford and Konigl 1979), bulk relativistic motion is ubiquitous in them. The observed flux density of the nuclear component is then Doppler-boosted at small angles of the motion to the line of sight, and differences between radio core-dominated (CDQs) and lobe-dominated quasars (LDQs) are due to orientation alone. The core-dominance parameter, R (the ratio of the radio flux density from the nucleus to that from the radio lobes) is then a statistical measure of the angle of inclination of the nuclear jet to the line of sight (Kapahi and Saikia 1982; Orr and Browne 1982). Interpreting correlations of X-ray luminosity with nuclear and lobe radio luminosities in this framework, Browne and Murphy (1987) suggested that a component of the X-ray emission in RLQs is orientation dependent.

The soft X-ray slopes have been found to be systematically flatter for core-dominated quasars than for lobe-dominated quasars; (Canizares and White 1989; Boroson 1989; Shastri 1991). Based on this trend, Shastri (1991) suggested that the "radio-linked" component of the X-ray emission (Zamorani *et al.* 1981; Kembhavi *et al.* 1986; Wilkes and Elvis 1987) is probably relativistically beamed.

The values of the core-dominance parameter (R) determined at an observed frequency of 5 GHz for the RLQs in our sample are given in Table 2. Fig. 3 shows that the X-ray energy index for our larger sample correlates inversely with log R, except for two quasars that are highly discrepant (see below). A Spearman rank test shows the correlation to be significant at the 99.95% level (one-tailed test) without the discrepant objects, and at the 90% level if they are included. Note that we have excluded the one Compact Steep Spectrum quasar in the sample (3C 48:0134+329) from Fig. 3, because, in these objects the cores often show complex radio structure (Fanti *et al.* 1990) and interaction of the radio jet with the interstellar medium is believed to be significant (van Breugel *et al.* 1984). The brightness of the nuclear components must reflect this interaction, in which case the parameter R is not

a good measure of orientation.

In the framework of the unified interpretation, the correlation in Fig. 3 is either due to a flat-spectrum X-ray component dominating at face-on inclinations, or due to a steep-spectrum component dominating at edge-on inclinations. It certainly cannot be explained by the anisotropy of the steep "ultrasoft excess" (Wilkes and Elvis 1987), since such an anisotropy would go in the opposite sense if the emission is from a central disc as has been suggested, besides dominating in a lower energy range. On the other hand, as was argued in Shastri (1991), bulk relativistic motion of material emitting a flat-spectrum X-ray component, (such as the nuclear jet), would give the required anisotropy. This suggestion fits in with the picture of an additional, flat-spectrum X-ray component associated with the radio emission in RLQs (Zamorani *et al.* 1981; Kembhavi *et al.* 1986; Wilkes and Elvis 1987). X-ray emission from radio jets is not unknown. Burns *et al.* (1983) find very good spatial coincidence of structures of the jet in Centaurus A as observed in the radio and X-ray bands. Harris and Stern (1987) measure a position for the candidate X-ray jet feature in 3C 273 which is coincident with one of the optical jet features imaged by Fraix-Burnet and Nieto (1988) (the latter's feature B). Similar coincidence is reported for knots in M87 (Biretta, Stern and Harris 1991).

The above correlation with R would contribute to the correlation of X-ray slope with core radio-loudness found by Wilkes and Elvis (1987), since it turns out that the core radio-loudness is correlated with R for the RLQs in the sample.

The correlation in Fig. 3 is consistent with the inhomogeneous jet model of Ghisellini, Maraschi and Treves (1985), proposed for the non-thermal emission from BL Lac-type objects (also see Maraschi 1992). The model proposes two components of X-ray emission from the jet; the first is a synchrotron component from nearer the nucleus which has a steep spectrum, and is relativistically beamed but into a relatively wide angle. The second is an inverse Compton component from the outer regions of the jet, that has a flat spectrum and is beamed into a cone narrower than that of the first component, either because of higher bulk velocities or greater collimation in the outer regions of the jet. Thus the model predicts that the compound X-ray spectrum will flatten as orientation changes from more edge-on to face-on inclinations of the nuclear jet. In the unified scheme, this would translate to flattening of the observed X-ray spectrum with increase of radio core dominance, as seen in Fig. 3.

The trend in Fig. 3 is inconsistent with the scenario of Melia and Konigl (1989) within the unified scheme. In the context of explaining BL Lac-type objects they proposed that the hard X-ray component is due to the inverse Compton "drag" on the relativistic jet by the thermal radiation from the nuclear disc near the nucleus, and the steep spectrum component is direct synchrotron emission from further out in the jet. The hard component is more isotropic than the steep spectrum component. It follows that the steep spectrum component would then dominate at face-on orientations, and the unified scheme would predict that the steep X-ray component dominate at large R values, opposite to that seen in Fig. 3.

Tests in the framework of the unified interpretation are most meaningful when the RLQs are chosen to have a narrow spread in an orientation-independent parameter. A study to test the above result with a sample of RLQs matched with respect to their radio lobe luminosities is underway with ROSAT. We note however that no trend of X-ray slope with radio lobe luminosity is indicated for the present sample.

It is suggestive that two of the quasars with amongst the lowest R values have nominally flat X-ray slopes (although with large uncertainties). We speculate that at the most edge-on inclinations of the quasar the steep-spectrum X-ray component may be occulted (by an obscuring torus?), leaving the residual flat-spectrum component that originates from further out in the jet still visible.

5 X-ray spectral slopes and the optical FeII emission

Wilkes, Elvis and McHardy (1987) suggested a correlation between the equivalent width of the FeIIλ4570 emission line strength and the soft X-ray slope for 9 quasars. This was later disputed, however, by Boroson (1989) and Zheng and O'Brien (1990), after finding no correlation for samples of 15 and 33 quasars respectively. Boroson (1989) claimed that the inconsistency with Wilkes, Elvis and McHardy (1987) was due to a combination of samples being different and measurements being inconsistent, while Zheng and O'Brien (1990) claimed that it was their equivalent width measurements of 3 additional quasars that destroyed the correlation.

Here we present our measured FeIIλ4570 emission line strengths for 18 of the present sample of quasars. Optical spectrophotometry was obtained for all the quasars on the Multiple Mirror Telescope during the years 1985-1988. Full observational details are given in Elvis *et al.* (1992). The strength of the FeIIλ4570 blend was measured above a linear continuum between the continuum region immediately longwards of H$\gamma\lambda$4340 and shortwards of H$\beta\lambda$4861. The HeIIλ4686 emission line is included in this measurement, unless noted, since deblending is highly inaccurate for such heavily blended lines. HeII is a high ionization line, probably from different gas than FeII, and thus its inclusion is likely only to add scatter into any relation followed by the FeII. We note that, if the emission line widths are >6000km s^{-1}, the continuum level estimate is likely to be high as the hydrogen line wings blend into those of the FeII emission (Wills 1988). Our sample was thus selected to include only quasars with lines narrower than 6000 km s^{-1} (with the exception of PG1613+658 where the continuum level is clear despite the large FWHM of 7050 km s^{-1}). The rest frame equivalent widths as derived from our measurements are listed in Table 1 for the RQQs and Table 2 for the RLQs.

Fig. 4a shows the FeII equivalent width plotted against the soft X-ray energy index. RQQs, CDQs (R > 0.5) and LDQs (R $\leq$ 0.5) are marked separately. The correlation between FeII strength and α_E is significant at the 99% level (Spearman rank test) for the full sample or for RQQs alone, although it is clear from the figure that the RLQs show no trend. PG1416-129 has a very flat spectral index in *Ginga* observations (0.05$\pm$0.15, Turner *et al.* 1989). Given the poor constraints on the *Einstein* value (0.9$\pm$0.5, 68% confidence range), the two results are consistent (the difference being $< 2\sigma$). If the *Ginga* value is used in preference (indicated by a filled square in Fig. 4a), the correlation is further strengthened (significance >99.5%).

The same scatter plot with FeIIλ4570 equivalent width data from Zheng and O'Brien (1990) shows a very similar trend (Fig. 4b). There is no significant correlation for the sample as a whole (as indeed is asserted by the authors), nor for the RLQs, but the RQQs show a trend similar to Fig. 4a (significance >95%). There appear to be no major inconsistencies

between their measurements and estimation procedure and ours. However, there remains one highly discrepant RQQ, 2130+099 (also in the sample of Boroson 1989, but not in our sample) which has strong FeII emission but an intermediate soft X-ray slope (0.8).

The data of Boroson (1989) do not show a correlation even for the RQQs. He uses the equivalent width of a different FeII multiplet ($\lambda\lambda$5105-5395)Å, but claims that his results cannot be different as a result of this, since there is a tight correlation between the FeII$\lambda\lambda$5105-5395 Å and FeII$\lambda\lambda$4500-4680Å equivalent widths. 14 of Boroson's objects have data in either Zheng and O'Brien (1990) or in Tables 1/2, or both. Of these, for 7 objects, the equivalent width measurements are broadly consistent with the present measurements and/or those of Zheng and O'Brien (1990); for the remaining 7, however, (including 4 RQQs), the equivalent widths of Boroson (1989) are highly discrepant. The reasons for this discrepancy are unclear. Possibilities include low signal-to-noise spectra causing large errors in the measurement, and variability.

While the high energy X-ray energy indices determined by *Ginga* do not by themselves show any significant correlation with the FeII equivalent width (Williams *et al.* 1992), the data for RQQs (available for 5 objects) are broadly consistent with Fig. 4a.

Standard photoionization models for the line emission from the Broad Line Regions of quasars (Krolik 1988) imply a close link between the spectral index of the ionizing X-ray continuum and the strength of the Fe emission lines. In the case of the RLQs, however, if the soft X-ray emission has a significant contribution from the jet as has been discussed above, then the X-ray energy index would not be a good indicator of the spectrum of the ionizing continuum. The absence of a correlation between the line strengths and the X-ray slope for RLQs would therefore be expected. Although there is a correlation for the RQQs, it is in the opposite sense to that predicted by the standard model in which the FeII emission is generated deep within the cloud and thus is sensitive to harder X-rays. It should be kept in mind though, that the standard models fail to predict the large strength of the optical FeII emission lines. Also, Zheng and O'Brien (1990) find a strong relation between the strength of the optical FeII emission and the Hβ FWHM. They compare their data with the simulations of Wills (1988) and conclude that the correlation cannot be explained by overestimation of the continuum alone. They suggest that the geometry of the emitting regions may also play a role in determining the observed FeII equivalent widths as discussed by Netzer, Laor and Gondhalekar (1992) and references therein. It is possible that geometry plays a role in the observed X-ray energy index as well, just as it appears to do in the RLQs. No correlation between X-ray slope and Hβ FWHM is seen in the current sample although, as noted above, the full range of FWHM is not included here to avoid measurement problems.

6 The range of X-ray slopes

The existence of correlations of the X-ray spectral index with external parameters in both the radio-quiet and radio-loud sub-samples allows us to strengthen the significance of the IPC measurements.

In the case of the RQQs the equivalent widths of the FeII lines are entirely independent of the X-ray measurement so the correlation of Fig. 4a can exist only if the soft X-ray slopes have a real intrinsic range of slopes from $\sim$0 to $\sim$1.5. This truly is a large range. It is, for

example, $\pm 4\sigma$ either side of the HEAO-2/EXOSAT mean, given the dispersion measured in those samples (Petre *et al.* 1984, Turner and Pounds 1989). Since our sample is small and incomplete, we cannot determine the real distribution of the slopes; the extremes we observe, however, cannot be rare.

Some active galactic nuclei have been discovered with the optical spectrum completely dominated by FeII emission (Lawrence *et al.* 1988). Soft X-ray observations of these AGN will test the FeII/soft-X-ray-slope relation in extremis, and may uncover some of the softest AGN. The alternative possibility is to measure FeII strengths in AGN selected to have particularly soft spectra, e.g., those in the 'Ultra-Soft Survey' of Cordova *et al.* (1989).

For the radio-loud sample a slightly smaller range of soft X-ray spectral index is required, $\sim 0 - 1$, to produce the observed correlation of X-ray slope and core dominance. This correlation is immediately subject to interpretation in the beaming hypothesis, as discussed above.

A wide spread of soft X-ray spectral indices for RQQs and RLQs is clearly required by their correlation with extrinsic parameters which themselves show extended ranges. For the RQQs, this implies the existence of (at least) another variable which affects their X-ray properties. This variable is at present unknown.

7 Conclusions

Using updated soft X-ray slopes for a sample of 45 quasars, we conclude the following:

- The earlier trend that radio-loud quasars have systematically flatter power-law fits to the soft X-ray spectrum than radio-quiet quasars is confirmed.
- The lack of a significant trend when each class is considered separately implies that they belong to two separate populations.
- For the radio-quiet quasars, soft (0.2-3.5 keV) X-ray slopes are consistent with those at higher (2-10 keV) energies for radio-quiet quasars but steeper than the high energy slopes of Seyfert 1 galaxies where reflection of the X-rays gives a good fit to the data.
- For the radio-loud quasars, X-ray slope correlates with the radio-core dominance. Within the framework of the unified interpretation this result suggests that a flat spectrum X-ray component dominates due to Doppler enhancement when the quasar jet is pointed towards us.
- A significant correlation exists between the FeII optical emission line strengths and X-ray spectral index for 11 radio-quiet quasars from our sample. Radio-loud quasars do not follow the correlation, consistent with the predominance of an extra X-ray component associated with the radio jet. The correlation demonstrates a close observational link between quasar emission lines and the observed X-ray continuum which is thought to excite them. However, most current photoionization models predict a correlation in the opposite sense, with the FeII generated deep inside the emitting clouds where only harder X-rays penetrate.

- The fact that the soft X-ray energy indices correlate with independent properties (core-dominance for RLQs and FeII equivalent widths for RQQs) argues for the wide range in the X-ray slopes of both classes being real.

8 Acknowledgements

The authors would like to thank Beverley J. Wills for her comments. P. Shastri acknowledges support from the NSF grant AST-8714937 and NASA grant NAG 5-1700. M. Elvis, B.J. Wilkes and J. McDowell acknowledge support of the NASA grant NAGW5-2201 (SARP) and contracts NAS8-30751 (HEAO-2) and NAS5-30934 (RSDC).

9 References

Arnaud, K. A., *et al.*, 1985, *MNRAS* **217**, 105.
Blandford, R. D. and Konigl, A., 1979, *ApJ* **232**, 34.
Biretta, J. A., Stern, C. P., and Harris, D. E. 1991, *AJ* **101**, 1632
Boroson, T. A., 1989, *ApJ* **343**, L9.
Browne, I. W. A. and Murphy, D. W., 1987, *MNRAS* **226**, 601.
Burns, J. O., Feigelson, E. D. and Schreier, E. J., 1983, *ApJ* **273**, 128.
Canizares, C. R. and White, J. L., 1989, *ApJ* **339**, 27.
Comastri, A., Setti, G., Zamorani, G., Elvis, M., Giommi, P., Wilkes, B. J. and McDowell, J. C., 1992, *ApJ* **384**, 62.
Cordova, F. A., Kartje, J., Rodriguez-Bell, T., Mason, K. O., and Harnden, F. R., 1989, in *Extreme Ultraviolet Astronomy*, eds. R. F. Malina and S. Bowyer, (New York: Pergamon Press), p. 30.
Elvis, M., Green, R. F. Bechtold, J., Schmidt, M., Neugebauer, G., Soifer, B. T., Matthews, K. and Fabbiano, G., 1986, *ApJ* **310**, 291
Elvis, M., Wilkes, B. J., McDowell, J. C., Green, R. F. Bechtold, J., Willner, S. P., Cutri, R., Oey, M., S., and Polomski, E. 1992, *ApJS in preparation*
Fanti, R., Fanti, C., Schilizzi, R. T., Spencer, R. E. Nan Rendong, Parma, P., van Breugel, W. J. M. and Venturi, T., 1990, *A&A* **231**, 333.
Fraix-Burnet, D. and Nieto, J.-L., 1988, *A&A* **198**, 87.
Ghisellini, G., Maraschi L., and Treves, A., 1985, *A&A* **146**, 204.
Harris, D. E. and Stern, C. P., 1987, *ApJ* **313**,136.
Johnson, H. L., 1966, *Ann. Rev. Astr. Ap.*, **4**, 193.
Kapahi, V. K. and Saikia, D. J., 1982, *J. Ap. & Astr.* **3**, 465.
Kembhavi, A., Feigelson, E. D., and Singh, K. P., 1986, *MNRAS* **220**, 51.
Krolik, J. H. 1988, in *Supermassive blackholes*, ed. Kafatos, M., (Cambridge: Cambridge University Press), p. 279.
Lawrence, A., Saunders, W., Rowan-Robinson, M., Crawford, J., Ellis, R. S., Frenk, C. S., Efstathiou, G., and Kaiser, N., 1988, *MNRAS* **235**, 261.

Maraschi, L., 1992, in *Variability of Blazars*, eds. E. Valtaoja and M. Valtonen, (Cambridge: Cambridge University Press), p. 447.

Masnou, J.-L., Wilkes, B. J., Elvis, M., Mcdowell, J. C., and Arnaud, K. A., 1992, *A&A* **253**, 35.

Melia, F. and Konigl, A., 1989, in *BL Lac Objects*, eds., L. Maraschi, T. Maccacaro and M.-H. Ulrich, 1989, (Berlin: Springer- Verlag) p. 372.

Mushotzky, R. F., 1984, *Adv. Sp. Res.*, **3**, 157.

Orr, M. J. L. and Browne, I. W. A., 1982, *MNRAS* **200**, 1067.

Netzer, H., Laor, A. and Gondhalekar, P. M. 1992, *MNRAS* **254**, 15.

Peacock, J. A., Miller, L. and Mead, A. R. G., 1986, in *IAU Symposium No. 119: Quasars* eds., G. Swarup and V. K. Kapahi, (Dordrecht: Reidel), p. 103.

Petre, R., Mushotzky, R. F., Krolik, J. H. and Holt, S. S., 1984, *ApJ* **280**, 499.

Pounds, K. A., Nandra, K, Stewart, G. C. George, I. M., and Fabian, A. C. 1990, *Nature*, **344**, 132.

Shastri, P. 1991, *MNRAS* **249**, 640.

Smith, E. P. and Heckman, T. M., 1990, *ApJ* **348**, 38.

Turner, M. J. L., Williams, O. R., Saxton, R., Stewart, G. C., Courvoisier, T. J.-L., Ohashi, T., Makishima, K., Kii, T. and Inoue, H., 1989. in *Proceedings of the 23rd ESLAB Symposium*, Vol. **2**, eds. J. Hunt and B. Batrick, (Noordwijk: ESA Publications Division), p. 769.

Turner, T. J. and Pounds, K. A. 1989, *MNRAS* **240**, 833.

van Breugel, W., Miley, G., and Heckman, T. M., 1984. *AJ* **89**, 5.

Wilkes, B. J. and Elvis, M., 1987 *ApJ* **323**, 243.

Wilkes, B. J., Elvis, M. and McHardy, I., 1987 *ApJ* **321**, L23.

Williams, O. R., Turner, M. J. L., Stewart, G. C., Saxton, R. D., Ohashi, T., Makishima, K., Kii, T., Inoue, H., Makino, F., Hayashida, K. and Koyama, K., 1992, *ApJ* **389**, 157.

Wills, B. J., 1988, in *Physics of Formation of FeII Lines Outside LTE*, eds., R. Viotti, A. Vittani, and M. Freidjung, (Dordrecht: Reidel), p. 161.

Zamorani, G. *et al.*, 1981, *ApJ* **245**, 357.

Zheng, W. and O'Brien, P. T., 1990, *ApJ* **353**, 433.

10 Figure Captions

Fig. 1a. The distribution of the radio-loudness parameter (R_{L_t}) for the quasars in our sample. (For the definition of radio-loudness see Section 2.)
Fig. 1b. The distributions of soft X-ray energy index α_E of the radio-loud (solid line) and radio-quiet (dashed line) quasars in our sample.
Fig. 2. The radio-loudness parameter (R_{L_t}) (Section 2) plotted against the soft X-ray energy index for the RLQs (filled squares) and RQQs (filled triangles) in the sample. The typical 1 σ error in the X-ray energy index is shown.
Fig. 3. For the RLQs, the soft X-ray energy index α_E plotted against the logarithm of the radio core-dominance parameter R (Section 3).
Fig. 4a. The rest frame equivalent width of the FeIIλ4570 multiplet plotted against the soft X-ray energy index α_E. Separately shown are RQQs (filled triangles), CDQs (crossed squares) and LDQs (empty squares). The single filled square is the *Ginga* measurement for 1416-129, whose IPC measurement has large errors. The dashed line represents a simple regression on the RQQ data to allow comparison with Figure 4b.
Fig. 4b. The same plot as in 4(a) but for the data from Zheng & O'Brien (1990). The symbols are as in 4(a). The Compact Steep Spectrum (CSS) object is 0134+329 (3C48). The regression line from Fig 4a is shown for comparison.

Table 1: Radio-quiet Quasars

Source	Other Name	Redshift	f_B^a mJy	R_{L_t}	α_E $(\pm 1\sigma)$	Ref.[c] (α_E)	W_λ^b(FeII) (Å)	Ref.[c] (W_λ)	FWHM(Hβ)[d] km s^{-1}
0026+129	PG	0.142	2.33	0.34	$0.88^{+0.05}_{-0.05}$	4			
0054+144	PHL909	0.171	1.02	-0.01	$0.41^{+0.07}_{-0.07}$	4			
0205+024	NAB	0.155	2.25	-0.18	$1.2^{+0.07}_{-0.07}$	4			
0844+349[f]	PG	0.064	11.15	-1.56	$1.6^{+0.7}_{-0.2}$	2	46	1,2	3380
0923+129[f]	PG	0.028	4.74	0.32	$0.7^{+0.3}_{-0.2}$	2	29	2	1840
1116+215	PG	0.177	3.80	-0.13	$1.0^{+0.3}_{-0.2}$	3	15	1	4290
1202+281	GQComae	0.165	2.33	-0.45	$1.1^{+0.2}_{-0.4}$	3,6			
1211+143	PG	0.085	6.24	1.40	$1.8^{+0.3}_{-0.2}$	3	32[e]	1,2	3000
1219+755	Mkn205	0.070	2.46	-0.31	$0.78^{+0.03}_{-0.03}$	4			
1229+204	Ton 1542	0.064	2.63	-0.59	$1.5^{+0.2}_{-0.1}$	2	45	2	3170
1244+026	PG	0.048	1.54	-0.27	$1.6^{+0.7}_{-0.5}$	3,6			
1304+346	AB133	0.189	0.50	-0.58	$1.0^{+0.6}_{-0.2}$	1			
1307+085	PG	0.158	3.43	-0.99	$0.9^{+0.5}_{-0.2}$	3,6	<8	1	5570
1407+265	PG	0.944	2.27	0.54	$1.2^{+0.9}_{-0.2}$	3			
1416-129	PG	0.129	3.07	0.07	$0.9^{+0.5}_{-0.5}$	3	<3	1	4640
1426+015	PG	0.086	3.66	-0.48	$1.2^{+0.2}_{-0.2}$	3	>20	1	5540
1501+106	Mkn841	0.036	7.04	-0.67	$0.93^{+0.04}_{-0.04}$	4	26[e]	1	5360
1613+658	PG	0.129	2.42	0.10	$1.1^{+0.2}_{-0.3}$	3	16	1	7050
1803+676	KAZ102	0.136	1.70	-0.69	$-0.2^{+0.4}_{-0.3}$	3	< 0.2	1,2	4810
2130+099	PG,IIZw136	0.061	4.78	-0.37	$0.81^{+0.07}_{-0.07}$	4			
2251-178	MR	0.068	4.48	-0.15	$0.3^{+0.5}_{-0.6}$	1			

a: f_B is calculated from B using $m_B(0)$=4440 Jy (Johnson 1966). When B magnitudes were not available, V magnitudes were used.
b: Equivalent width of FeIIλ4570 in the quasar's rest frame (uncertainites are $\sim \pm 10\%$).
c: References: (1) this paper; (2) Wilkes, Elvis and McHardy 1987; (3) Wilkes and Elvis 1987; (4) Masnou *et al.* 1992; (5) Elvis *et al.* 1992; (6) Elvis *et al.* 1986.
d: Full width at half-maximum of Hβ in the observed frame.
e: HeIIλ4686 excluded from measurement.
f: Errors on α_E are scaled to 1σ from the 90% errors given in Wilkes, Elvis and McHardy (1987).

Table 2: Radio-loud Quasars

Source	Other Name	Redshift	f_B mJy	R_{L_t}	R	α_E $(\pm 1\sigma)$	Ref.[c] (α_E)	W_λ^b (Å)	Ref.[c] (W_λ)	FWHM[d] km s^{-1}
0007+106	III Zw 2	0.089	1.83	2.24	0.9	$0.4^{+0.9}_{-0.3}$	3	5	2	4700
0133+207	3C 47	0.425	0.24	3.65	0.07	$0.9^{+0.3}_{-0.3}$	3			
0134+329	3C 48	0.367	1.40	3.61	CSS	$0.7^{+0.4}_{-0.4}$	3			
0312-770	PKS	0.223	1.39	2.60	10.9	$0.1^{+0.6}_{-0.2}$	3	18	2	3340
0637-752	PKS	0.656	1.64	3.53	>10	$0.5^{+0.1}_{-0.1}$	4			
0837-120	3C206,PKS	0.198	2.16	2.58	0.3	$0.6^{+0.3}_{-0.3}$	5	<8	1	4485
0903+169	3C 215	0.411	0.18	3.36	0.05	$0.0^{+0.6}_{-0.2}$	3			
0923+392	4C 39.25	0.699	0.30	4.39	36	$0.4^{+0.2}_{-0.1}$	3			
1020-103	PKS	0.197	1.40	2.44	5.5	$0.8^{+0.7}_{-1.6}$	1			
1028+313	B2	0.177	0.66	2.38	1.3	$0.62^{+0.06}_{-0.06}$	4	< 3	1	4280
1100+772	3C 249.1	0.311	2.33	2.52	0.1	$1.0^{+0.3}_{-0.5}$	3			
1111+408	3C254	0.734	0.25	3.50	0.02	$1.0^{+0.9}_{-0.3}$	1			
1128+315	B2	0.289	1.02	2.39	9.6	$0.7^{+0.5}_{-0.4}$	1			
1137+660	3C 263	0.656	1.12	2.97	0.2	$0.7^{+0.4}_{-0.1}$	3			
1146-037	PKS	0.341	0.73	2.37	1.4	$0.3^{+0.5}_{-0.2}$	3	3	2	4300
1217+023	PKS	0.240	1.07	2.64	2.0	$0.5^{+0.3}_{-0.1}$	3			
1226+023	3C 273	0.158	26.27	3.12	5.5	$0.47^{+0.03}_{-0.03}$	4	15	1,2	4300
1253-055	3C 279	0.538	0.28	4.58	7.8	$0.6^{+0.1}_{-0.2}$	3			
1545+210	3C 323.1	0.266	0.85	3.04	0.05	$0.8^{+0.3}_{-0.5}$	3,6			
1635+119	MC	0.146	0.72	2.05	0.3	$0.9^{+1.0}_{-0.6}$	3			
1704+608	3C351	0.371	3.04	2.60	0.02	$0.1^{+0.9}_{-0.5}$	5	3[e]	1	2420
1721+343	4C 34.47	0.206	1.12	2.76	1.2	$0.5^{+0.4}_{-0.3}$	3			
2128-123	PKS	0.501	2.49	2.92	>20	$0.5^{+0.8}_{-0.3}$	1			
2135-147	PKS	0.200	1.77	2.99	0.09	$0.73^{+0.05}_{-0.05}$	4			

a: f_B is calculated from B using $m_B(0)$=4440 Jy (Johnson 1966). When B magnitudes were not available, V magnitudes were used.

b: Equivalent width of FeIIλ4570 in the quasar's rest frame (uncertainites are $\sim \pm 10\%$).

c: References: (1) this paper; (2) Wilkes, Elvis and McHardy 1987; (3) Wilkes and Elvis 1987; (4) Masnou *et al.* 1992; (5) Elvis *et al.* 1992; (6) Elvis *et al.* 1986.

d: Full width at half-maximum of Hβ in the observed frame.

e: HeIIλ4686 excluded from measurement.

Authors' Addresses

M. Elvis, J. C. McDowell and B.J. Wilkes: Harvard-Smithsonian Center for Astrophysics, 60 Garden Street, Cambridge MA 02138.

P. Shastri: Astronomy Department, University of California, Berkeley CA 94720.

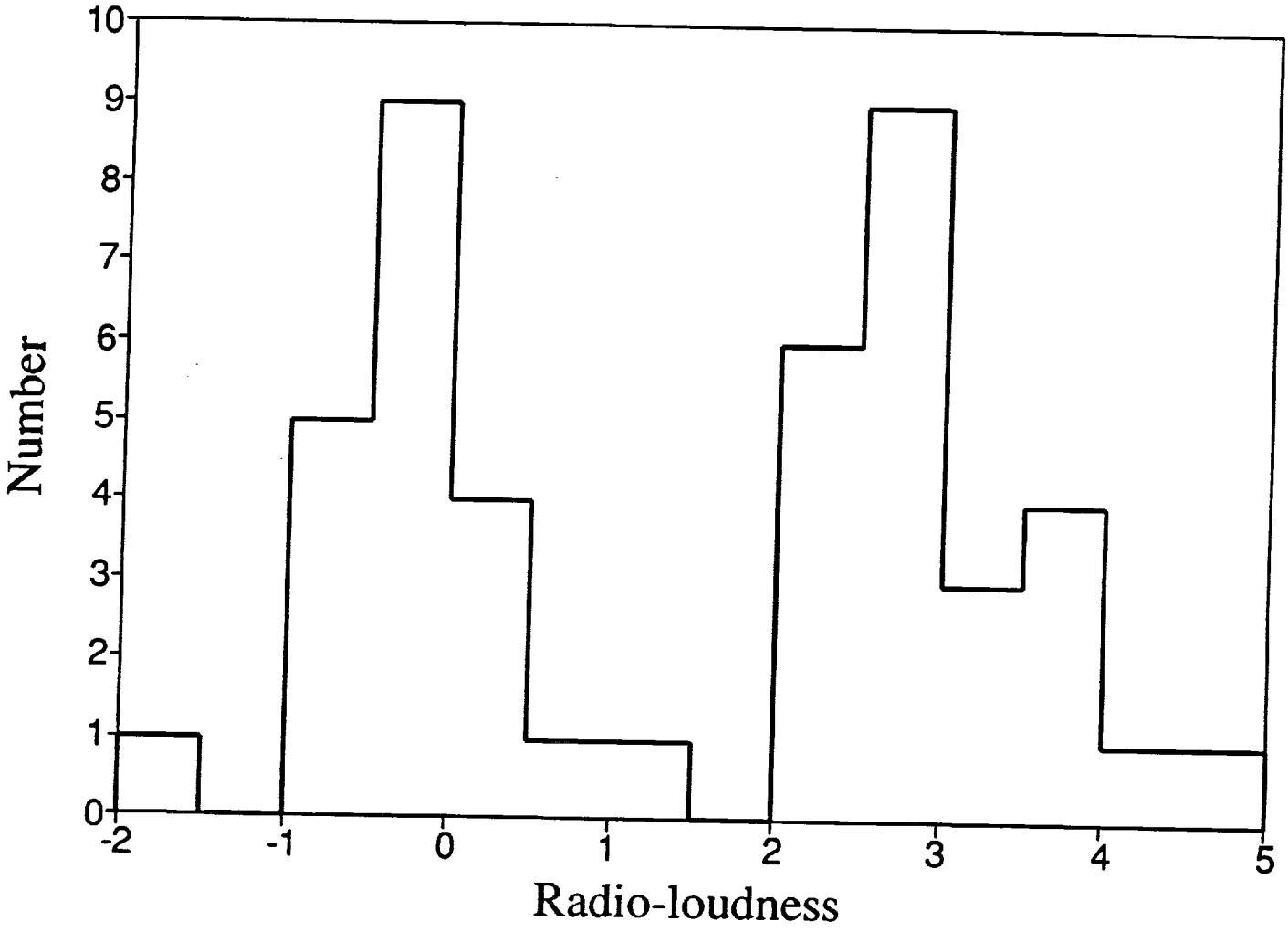

Figure 1a

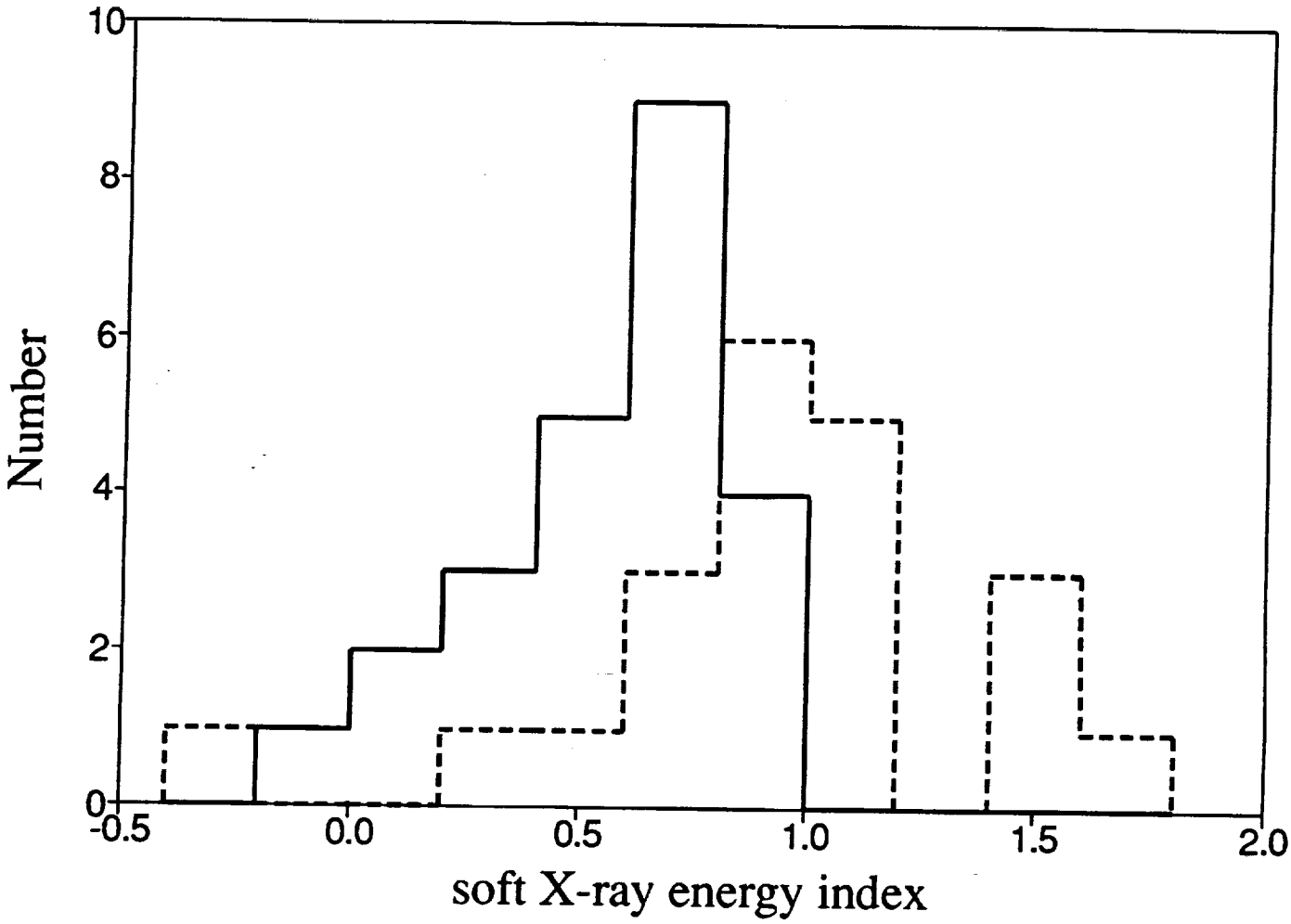

Figure 1b

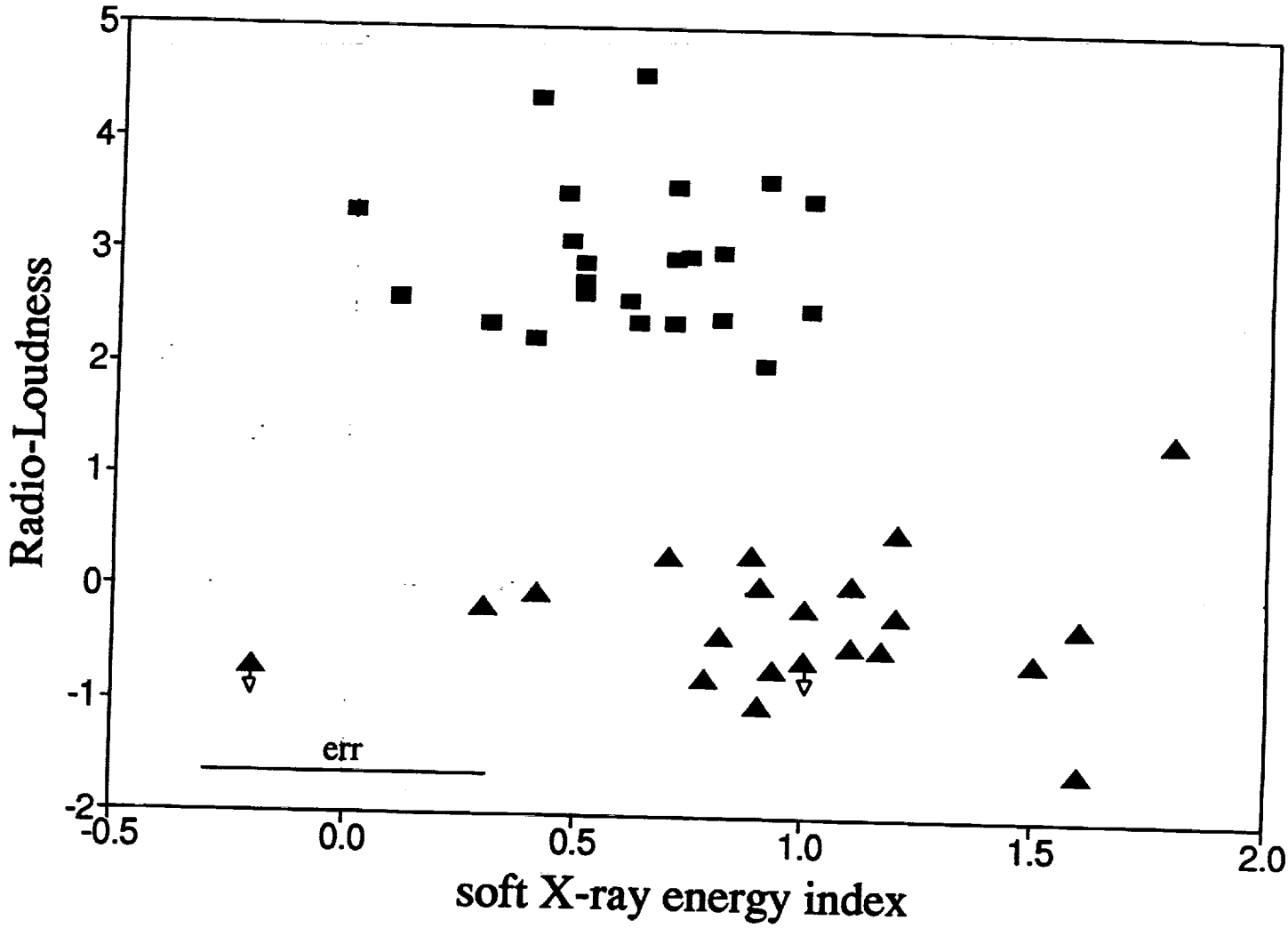
Radio-Loudness
soft X-ray energy index
err
5
4
3
2
1
0
-1
-2
-0.5
0.0
0.5
1.0
1.5
2.0

Figure 2

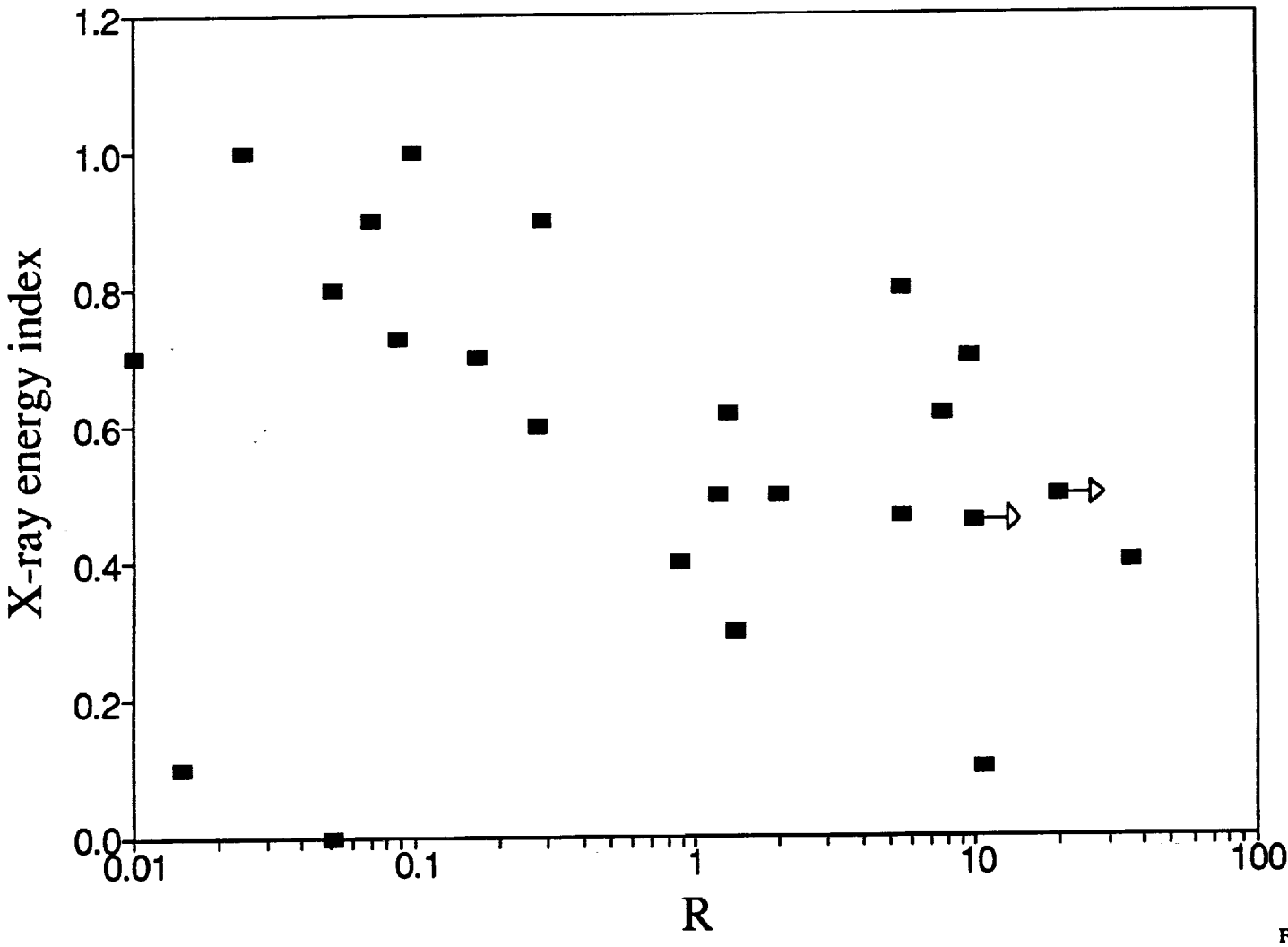

Figure 3

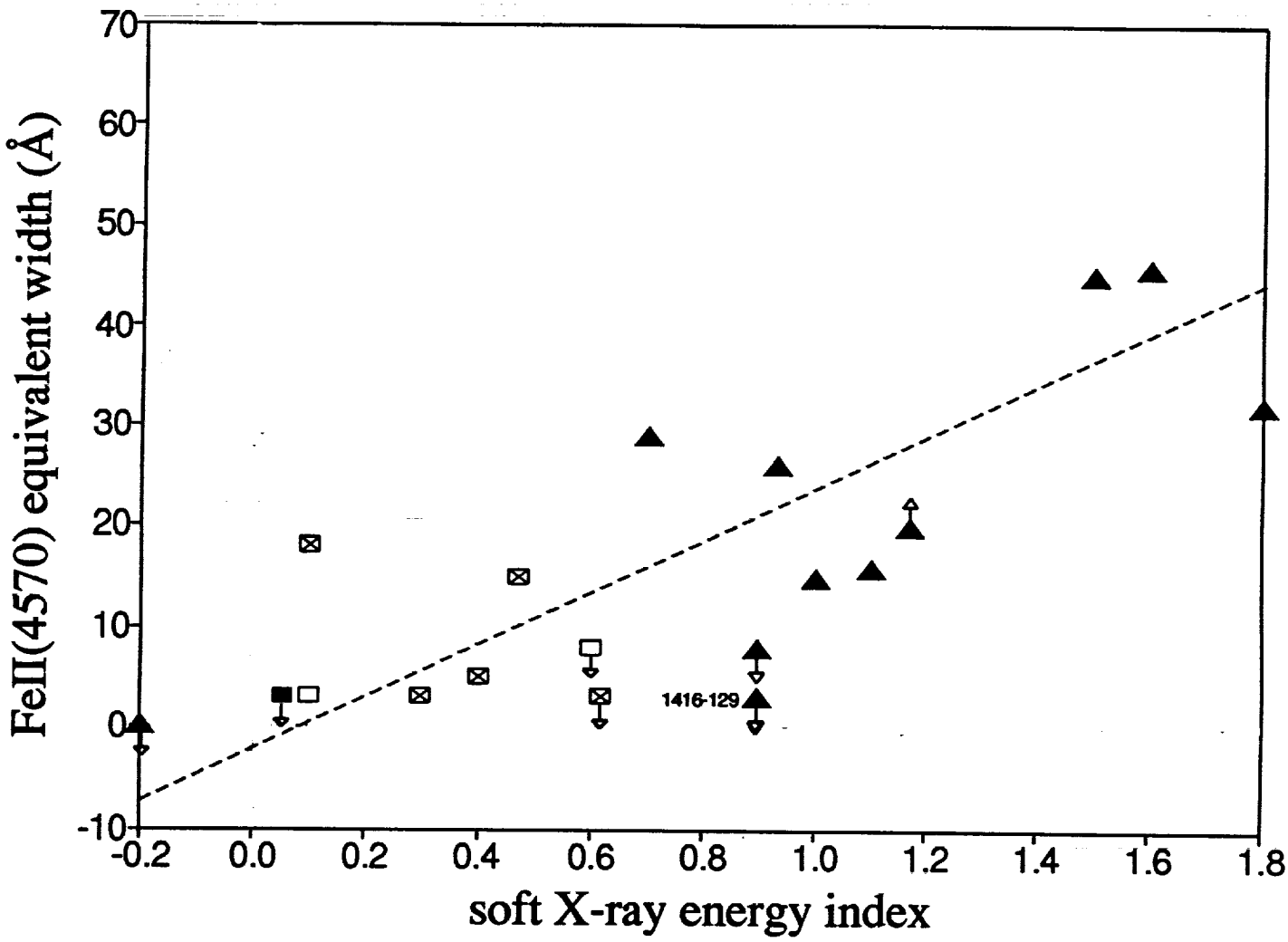
FeII(4570) equivalent width (Å)
70
60
50
40
30
20
10
0
-10
-0.2
0.0
0.2
0.4
0.6
0.8
1.0
1.2
1.4
1.6
1.8
soft X-ray energy index
1416-129

Figure 4a

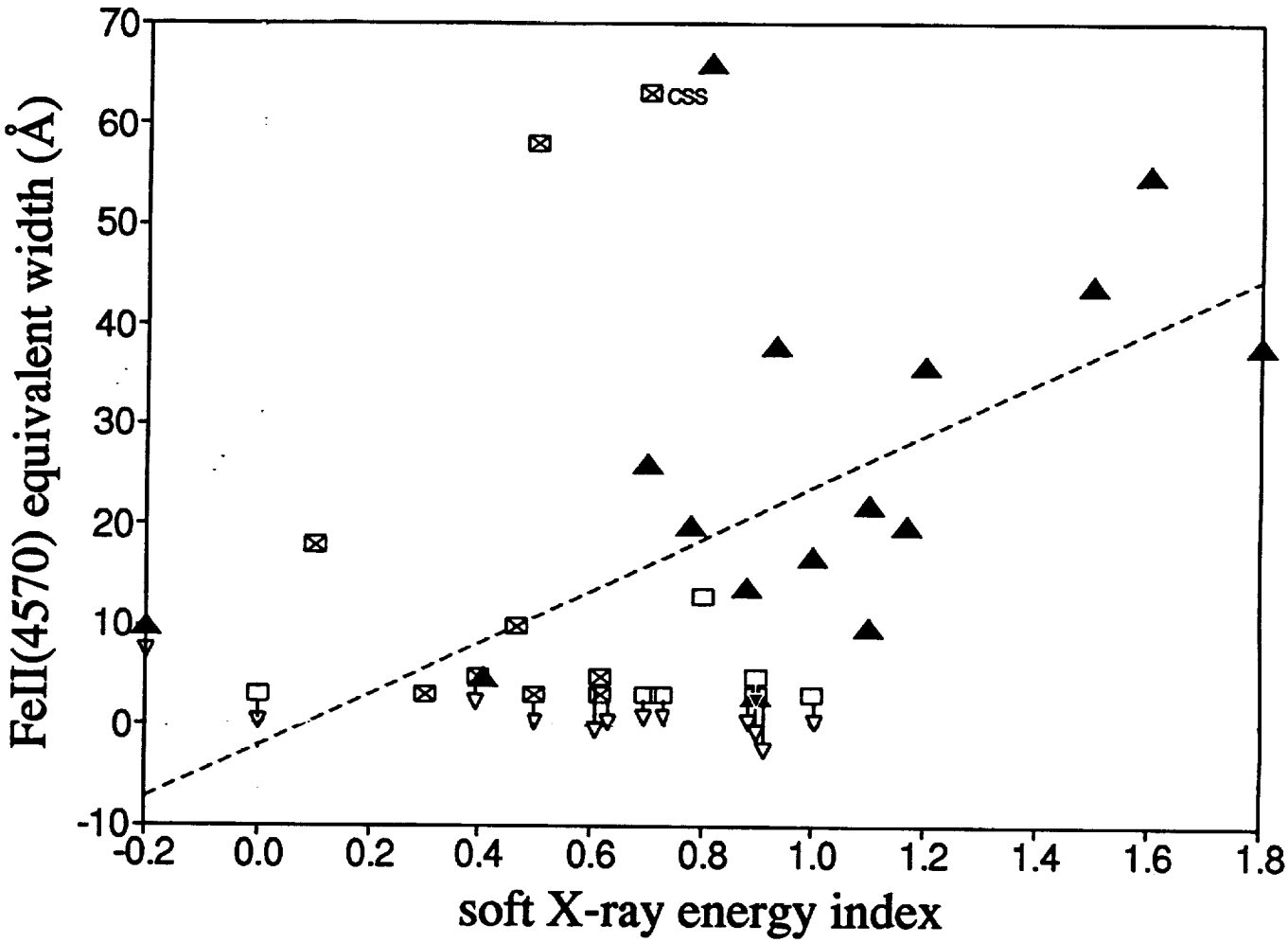
FeII(4570) equivalent width (Å)
soft X-ray energy index
CSS
70
60
50
40
30
20
10
0
-10
-0.2
0.0
0.2
0.4
0.6
0.8
1.0
1.2
1.4
1.6
1.8

Figure 4b